elevated P-gp expression [10]. Furthermore, Olaizola et al. reported that the uptake of [^{99m}Tc]-sestamibi (which is known to be a substrate of P-gp and is excreted by P-gp [11,12]) by the parathyroid glands of uremic patients was suppressed by pulse administration of 1,25-$(OH)_2D_3$ for 2 weeks, suggesting that P-gp induction by 1,25-$(OH)_2D_3$ leads to increased [^{99m}Tc]-sestamibi efflux [13].

The biological activity of 1,25-$(OH)_2D_3$ is mainly mediated via the vitamin D receptor (VDR), a member of the nuclear receptor superfamily. VDR forms a heterodimer with retinoid X receptor (RXR) and binds to the vitamin D response element (VDRE) in the regulatory region of genes. The VDRE by which the gene is regulated positively is generally composed of a direct repeat (DR) of the consensus hexamer (half-site) sequence of 5′-RGKTCA-3′ (R = A or G, and K = G or T) spaced by three or four nucleotides (DR3 or DR4), or an everted repeat spaced by 6, 7, 8, or 9 nucleotides (ER6, ER7, ER8, or ER9) [14–17]. However, negative response elements for 1,25-$(OH)_2D_3$ have been identified in several genes down-regulated by 1,25-$(OH)_2D_3$, such as human pituitary transcription factor-1 gene, in which an imperfect DR2 motif acts as a negative VDRE [18].

Previously, Geick et al. reported that the induction of *MDR1* by rifampin is mediated by PXR which binds to a DR4 located between −7.9 and −7.8 kbp upstream from the transcription start site [3]. Burk et al. reported that CAR also induces *MDR1* expression by binding to several DR4s located in the same region [4]. Recently, we reported that thyroid hormone receptor (TR) regulates the expression of *MDR1* by binding to several DRs located in the same region [19]. It was reported that 1,25-$(OH)_2D_3$ also regulates *CYP3A4* induction through the binding of VDR/RXRα to some PXR response elements [14]. These results suggest that VDR also binds to several DR motifs in the same region of the *MDR1* gene and regulates the expression of *MDR1*. However, this theory requires substantiation.

There is variation amongst individuals in intestinal *MDR1* expression [20]. Since 1,25-$(OH)_2D_3$ induces the expression of *MDR1*, the 1,25-$(OH)_2D_3$-mediated induction process might be involved in this inter-individual variation. Furthermore, vitamin D is widely prescribed and influences the induction of P-gp, which potentially affects pharmacokinetics. Therefore, the role of vitamin D in the mechanism of *MDR1* expression is worthy of investigation. In this study, we investigated that how 1,25-$(OH)_2D_3$ regulates the expression of *MDR1* using the intestinal epithelial cell line Caco-2. We demonstrate that the induction of *MDR1* by 1,25-$(OH)_2D_3$ is mediated by VDR/RXRα binding to several VDREs located between −7880 and −7810 bp upstream of the *MDR1* gene, in which every VDRE additively contributes to the 1,25-$(OH)_2D_3$ response.

2. Materials and methods

2.1. Plasmid constructs

Human VDR cDNA was amplified from human kidney Marathon-Ready cDNA (Clontech Laboratories Inc., Palo Alto, CA, USA) with the primers 5′-ATGGAGGCAATGGCGGC-3′ and 5′-TCAGGAGATCTCATTGCCAAACAC-3′ using a TaKaRa LA Taq (Takara Bio Inc., Shiga, Japan). The resulting DNA fragment was subcloned into the pEF6/V5-His-TOPO vector (Invitrogen, Carlsbad, CA, USA) and this expression plasmid (pEF6/V5-hVDR) was used for the transfection. The sequences were verified by DNA sequencing. The pEF6/V5-hVDR plasmid was digested with KpnI (Toyobo, Osaka, Japan) and NotI (Takara Bio Inc.), and the resulting fragment was ligated into the pCMVTNT expression plasmid (Promega, Madison, WI, USA), which was digested with KpnI and NotI. This plasmid (pCMVTNT-hVDR) was used for the in vitro synthesis. The expression plasmid encoding human RXRα cDNA (pcDNA3.1-hRXRα) was a generous gift from Dr. Shuichi Koizumi (Yamanashi University, Japan). Luciferase reporter gene plasmids containing various lengths of the human MDR1 5′-flanking sequence were previously constructed in our laboratory [19]. Mutations in several half-sites were introduced into the pMD*824Δ90L reporter plasmid using a QuikChange Multi Site-Directed Mutagenesis kit (Stratagene, La Jolla, CA, USA) according to the manufacturer's instructions, with the previously described oligonucleotides and the following oligonucleotides, used alone or in combination: M28, 5′-GCT-CCTGGGAGAGAGAACATTTGAGATTAAACAAG-3′; M31, 5′-GA-ACTAACTTGACCTTTTTCCTGGGAGAGAGTTC-3′; M33, 5′-AA-ATGAACTCAATCCCAGGAGCAAG-3′. For the M28, M29, M30, and M36 mutants shown in Fig. 4A, mutations were introduced into the M1, M3, M12, and M23 constructs using the M28 primer. For the M38 mutant shown in Fig. 4A, a deletion mutant was obtained by chance when we attempted to create the M30 mutant. All mutations were verified by DNA sequencing.

2.2. Cell culture

Caco-2 cells, a human colon adenocarcinoma cell line, were obtained from American Type Culture Collection (Manassas, VA, USA). Caco-2 cells were cultured in low glucose Dulbecco's modified Eagle's medium (DMEM, Sigma–Aldrich, St. Louis, MO, USA) supplemented with 10% heat-inactivated fetal bovine serum (FBS), 100 U/mL penicillin G/100 μg/mL streptomycin (Gibco-Invitrogen, Carlsbad, CA, USA), and 1× MEM non-essential amino acids solution (Gibco-Invitrogen) at 37 °C under 5% CO_2–95% air.

2.3. Transfection and luciferase reporter gene assays

Caco-2 cells were seeded into 96-well plates (1.6×10^4 cells/well), grown overnight, and transiently transfected using HilyMax (at a ratio of DNA to HilyMax of 1:5; Dojindo Laboratories, Kumamoto, Japan) according to the manufacturer's instructions with 10 ng/well of VDR expression plasmid (pEF6/V5-hVDR), 100 ng/well of the indicated luciferase reporter plasmid, and 10 ng/well of the *Renilla* luciferase reporter plasmid, pGL4.74 [hRluc/TK] (Promega) to normalize the transfection efficiency. After 24 h, the medium was replaced by phenol red-free DMEM (Gibco-Invitrogen) supplemented with 10% dextran-coated charcoal-stripped FBS (Hyclone Laboratories, Logan, UT, USA) containing 25 nM 1,25-$(OH)_2D_3$ (Sigma–Aldrich) or dimethyl sulfoxide (DMSO) for 3.5 h. Firefly and *Renilla* luciferase activities were measured using a Dual-Glo Luciferase Assay System (Promega) according to the manufacturer's instructions and a luminometer (Wallac 1420 ARVO sx Multilabel counter, PerkinElmer Life Sciences, Boston, MA, USA). Firefly luciferase activity was normalized to

Renilla luciferase activity, and the inducibility was calculated as the ratio of luciferase activity of 1,25-$(OH)_2D_3$-treated cells to that of control (DMSO-treated) cells. The results represent the mean ± S.D. of four independent experiments, and in each of these experiments the control and 1,25-$(OH)_2D_3$ treatments were performed at least in triplicate.

2.4. *Electrophoretic mobility shift assays (EMSAs)*

TNT T7 and SP6 Quick Coupled Transcription/Translation Systems (Promega) were used for in vitro synthesis of human RXRα protein from pcDNA3.1-hRXRα and human VDR protein from pCMVTNT-hVDR, respectively, according to the manufacturer's instructions. The plus strand sequences of probes and competitors used in EMSA are shown in Figs. 2A and 3A. The nonspecific competitor was double-stranded oligonucleotide located in the −218 to −117 region of the human PXR promoter [21]. The oligonucleotides, except for longer probes described below, were purchased from Sigma Genosys (Hokkaido, Japan) and equal amounts of complimentary strands were annealed. The longer probes, except for the 7882 probe shown in Fig. 3A, were prepared by polymerase chain reaction (PCR) amplification as described previously [19]. The reaction mixture used to obtain the results shown in Fig. 2B–D was prepared as follows: 2.5 μL aliquots of the in vitro translated proteins (VDR or RXRα alone, or mixed at a ratio of 1:1) or unprogrammed reticulocyte lysate were incubated for 20 min at room temperature with 1 μL of 5× binding buffer [15 mM $MgCl_2$, 0.5 mM EDTA, 2.5 mM dithiothreitol (DTT), 50% glycerol and 100 mM HEPES, pH 7.75], 0.5 μL of 1 mg/mL poly(dI–dC) (GE Healthcare UK Ltd., Buckinghamshire, UK), and 0.5 μL of 0.33 μM 5′-fluorescein isothiocyanate (FITC)-labeled double-stranded oligonucleotide probe. For competition assays, 0.5 μL of unlabeled oligonucleotide was simultaneously added to the reaction mixture with the probe. For the assays used to obtain the results shown in Fig. 3, 2–8 μL (Fig. 3B) or 8 μL (Fig. 3C) of the in vitro translated VDR and RXRα mixed at a ratio of 1:1 were used, if necessary, the volume of which was adjusted to 8 μL with unprogrammed reticulocyte lysate. The 8-μL aliquots of the proteins were incubated for 20 min at room temperature with 1 μL of 10× binding buffer (30 mM $MgCl_2$, 1 mM EDTA, 5 mM DTT, 50% glycerol and 200 mM HEPES, pH 7.75), 0.5 μL of 1 mg/mL poly(dI–dC), and 0.5 μL of the PCR-based probe or 0.33 μM 5′-FITC-labeled 7882 probe in the presence or absence of 250 nM 1,25-$(OH)_2D_3$. The 1.5-μL aliquots of the protein–DNA complexes were resolved by electrophoresis on 2.8 or 6% non-denaturing Long Ranger gels (Lonza, Basel, Switzerland) run in 0.5× TBE (44.5 mM Tris, 44.5 mM boric acid, and 1.25 mM EDTA) at 500 V constant voltage, and visualized and quantified on a slab gel DNA sequencer DSQ-2000L (Shimadzu Co., Kyoto, Japan).

3. Results

3.1. *Identification of the 1,25-$(OH)_2D_3$-responsive region in the MDR1 gene*

To investigate the mechanism of *MDR1* gene expression induced by 1,25-$(OH)_2D_3$, we performed a luciferase reporter gene assay using an intestinal epithelial cell line, Caco-2, which expresses VDR at relatively lower level [9]. The cells were transfected with a reporter plasmid containing the 5′-upstream region from −10082 to +117 bp of *MDR1* (pMD10082L) in the presence or absence of an expression plasmid encoding VDR. Following the treatment with either vehicle (DMSO) or 1,25-$(OH)_2D_3$, luciferase assays were performed. In the absence of VDR expression plasmid, 1,25-$(OH)_2D_3$ had little affect on the transcriptional activity. By contrast, in the presence of VDR expression plasmid, more than an eightfold activation was induced by 1,25-$(OH)_2D_3$ (Fig. 1A). These results indicate that the 1,25-$(OH)_2D_3$-responsive region is located within 10 kbp of the 5′-flanking region of *MDR1*, and that VDR mediates *MDR1* induction by 1,25-$(OH)_2D_3$.

Next, to identify the response elements implicated in the transcriptional regulation of *MDR1* by 1,25-$(OH)_2D_3$, we performed luciferase assays using several deletion mutants of pMD10082L. As shown in Fig. 1A, the 824 bp deletion from −7970 to −7145 bp resulted in the complete loss of inducibility. The lost inducibility was recovered by reinsertion of the deleted region of 824 bp (Fig. 1A, bottom line, pMD*824L). These results indicate that the 824 bp region is essential for the induction of *MDR1* by 1,25-$(OH)_2D_3$.

To further define the minimal region for the VDR response, deletion analysis was performed based on pMD*824L, which contains the 824 bp region (Fig. 1B). The 90 bp deletion from the 5′-end did not affect inducibility, whereas the 153 bp deletion from the 5′-end resulted in the complete loss of inducibility. These data suggest that the essential region for the VDR-mediated induction is located between −7880 and −7817 bp.

3.2. *VDR binds to the putative VDRE as a heterodimer with RXRα*

We scanned the 1,25-$(OH)_2D_3$ response region between −7880 and −7810 bp using the JASPAR FAM database (http://jaspar.genereg.net/). Several putative half-sites, a pair of which composes a DR or ER, were found (Hs1–8, Fig. 2A). Generally, some DRs or ERs, including DR3 and DR4 (which lie in this region, as shown in Fig. 2A) act as VDRE.

The region including the putative VDRE was divided into three segments, designated upstream cluster (UpC), middle cluster (MdC), and downstream cluster (DwC); we have reported this convenient classification previously [19]. Each cluster has several putative half-sites. To determine whether VDR and RXRα could bind directly to these segments, EMSA was performed using in vitro translated VDR and RXRα. The probes and competitors used for the EMSA are summarized in Fig. 2A. The DNA–protein complexes were formed in the presence of both VDR and RXRα, although the complexes were not formed in the absence of either protein, indicating that the protein complex VDR/RXRα binds to each segment (Fig. 2B–D). The DNA–protein complexes were competed out by the self-competitors but were not competed out by the nonspecific competitor (Fig. 2B–D). The relative affinities of VDR/RXRα to UpC, MdC, and DwC were further assessed by competition experiments. As shown in Fig. 2B, the complexes of UpC with VDR/RXRα were competed out by competitors UpC, MdC, and DwC. Of these, UpC was the most effective competitor for the formation of the DNA–protein complexes, and MdC inhibited

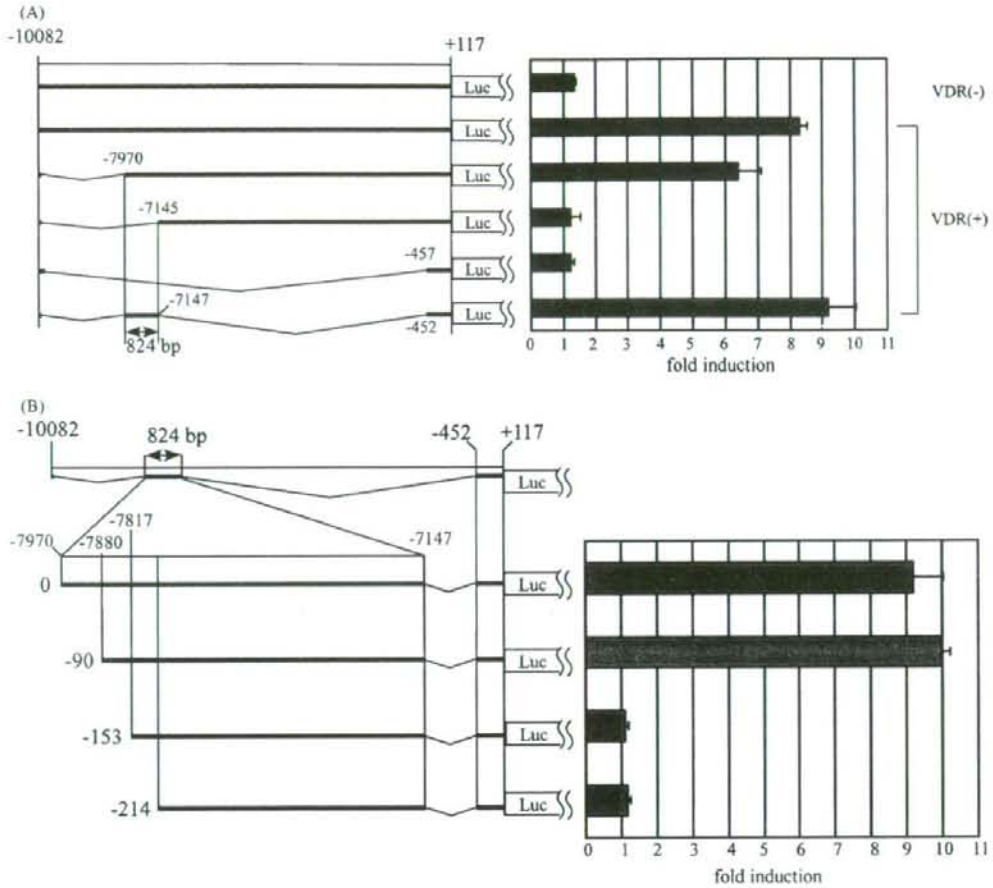

Fig. 1 – Transcriptional activity of several deletion mutants of human MDR1 in the 5′-upstream region induced by 1,25-$(OH)_2D_3$. The 5′-upstream region of the MDR1 gene was cloned into pGL4.12, as indicated on the left. Numbers are in reference to the transcriptional start site at +1. Luciferase activity was analyzed as described in Section 2. Fold induction was calculated as the ratio of luciferase activity in 1,25-$(OH)_2D_3$-treated cells to that of DMSO-treated cells, and is indicated on the right side of each column. Each value represents the mean ± S.D. of four independent experiments. (A) Schematic representations of pMD10082L, pMD7970L, pMD7145L, pMD457L and pMD*824L are shown from the top of the left side. (B) Schematic representations of pMD*824L, pMD*824Δ90L, pMD*824Δ153L, and pMD*824Δ214L are shown from the top of the left side.

complex formation to an extent similar to that of DwC (Fig. 2B). Similar competition assay results were obtained using MdC and DwC probes (Fig. 2C and D).

To identify the VDR/RXRα-binding site in these segments, shorter oligonucleotides containing two or three half-sites were used as competitors (Fig. 2B). The most efficient competitor for VDR/RXRα binding to UpC was DR4(I), followed by DR3, MdC3, DR4(III), and DR4(II). MdC5 lacking Hs6 of MdC was not able to compete for the UpC probe, indicating that Hs6 is necessary for MdC–VDR/RXRα binding.

Next, oligonucleotides including a set of 2 bp mutations in each of the half-sites (UpM1~DwM12 in Fig. 2A) were used as competitors for EMSA. As shown in Fig. 2B, UpM1 including the Hs1 mutation in UpC competed for the UpC probe at the same level as the wild-type competitor. UpM3 including the Hs3 mutation in UpC competed slightly less efficiently than the wild-type. UpM2 including the Hs2 mutation in UpC failed to compete for UpC, indicating that Hs2 is essential for UpC–VDR/RXRα complex formation (Fig. 2B).

The result obtained using the MdC probe is shown in Fig. 2C. To determine which half-site of MdC3 is required for MdC–VDR/RXRα complex formation, the mutant oligonucleotides including the 2 bp mutations in the half-sites of MdC3 were used as competitors (MdM31, M33, and M4). MdM31 including the Hs4 mutation partially competed for MdC, but MdM33 containing the Hs5 mutation competed for MdC as effectively as the wild-type competitor. MdM4 including the Hs6 mutation in MdC3 failed to compete for

the MdC probe, indicating that Hs6 is essential for MdC3–VDR/RXRα complex formation. This result is consistent with the fact that MdC5, which lacks Hs6 of MdC, is not able to bind VDR/RXRα.

The result obtained using the DwC probe is shown in Fig. 2D. The Hs6 and Hs7 mutations in DwC (DwM4 and DwM7, respectively) did not affect the competition for DwC, whereas the Hs8 mutation caused reduced competition by DwM12 for

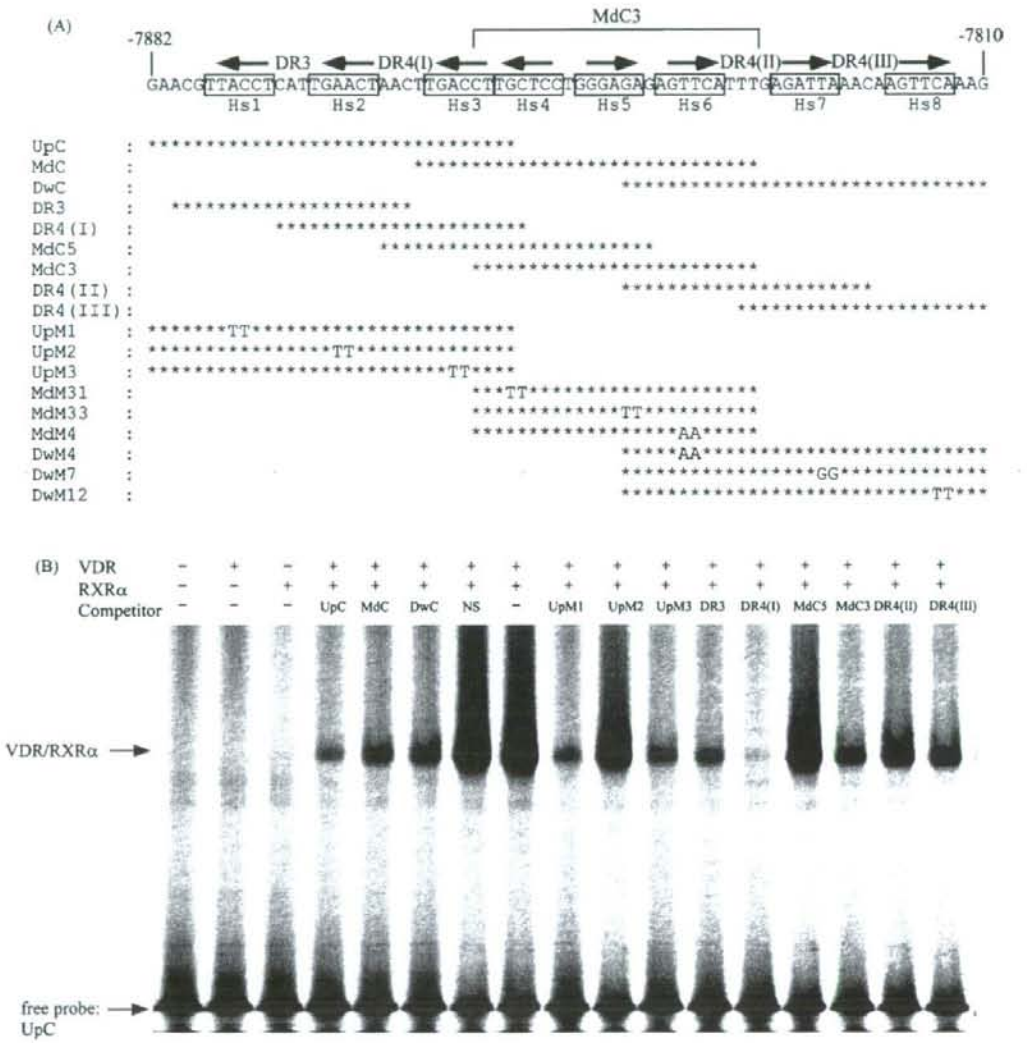

Fig. 2 – VDR binds to the putative VDREs in the region essential for VDR-mediated induction as a heterodimer with RXRα. (A) Oligonucleotide sequences used for EMSA. Putative half-sites (Hs1–8) predicted using JASPAR FAM are boxed, and arrows indicate the direction of the half-site. Numbers are in reference to the transcriptional start site at +1. Only nucleotides that differ from the wild-type are shown as letters; asterisks represent unchanged nucleotides. (B) EMSA was performed using a FITC-labeled UpC probe. The UpC probe was incubated in the absence or presence of in vitro translated VDR, RXRα, or both proteins, as described in Section 2. In parallel experiments, a competition assay was performed in the presence of a 50-fold molar excess of unlabeled oligonucleotide. "NS" indicates nonspecific competitor. The complexes were resolved by electrophoresis on a 6% Long Ranger gel. (C) EMSA was performed using a FITC-labeled MdC probe. The procedure was the same as that described in (B), except that a 15-fold molar excess of unlabeled oligonucleotides were used for the competition assay. "NS" indicates nonspecific competitor. (D) EMSA was performed using a FITC-labeled DwC probe. The procedure was the same as that described in (C). "NS" indicates nonspecific competitor.

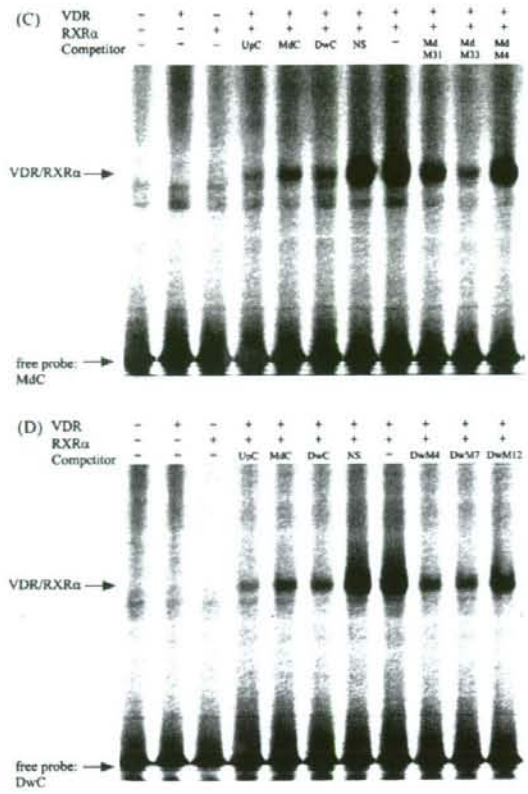

Fig. 2. (Continued).

the DwC probe. These results indicate that Hs8 is important for DwC–VDR/RXRα complex formation.

Taken together, VDR/RXRα is able to bind to several putative VDREs [DR4(I) and DR3 in UpC, MdC3 in MdC, and DR4(III) and DR4(II) in DwC] with different affinity. Additionally, Hs2, Hs6, and Hs8 are the most important half-sites in each segment for DNA–VDR/RXRα complex formation.

3.3. *Three molecules of VDR/RXRα are able to bind to the VDR-binding region at the same time*

Although we identified several sites competent to bind VDR/RXRα, the sites in this region are spaced relatively close to each other. The proximity of these VDR-binding sites might prevent the binding of VDR/RXRα to these sites. Therefore, the question that arises is how many molecules of VDR/RXRα bind to the VDR-binding region at the same time. To examine this, we performed EMSA using a longer probe (7882 probe in Fig. 3A) containing all the half-sites of the VDR-binding elements using different amounts of VDR/RXRα. At the highest concentration of the protein in the presence of 1,25-$(OH)_2D_3$, three shifted bands (upper, middle, and lower) were observed, although the intensity of the upper mobility band (3× VDR/RXRα in Fig. 3B) was weak. In the absence of 1,25-$(OH)_2D_3$, the upper band was very weak. The mobility of the lower band (1× VDR/RXRα in Fig. 3B) is the same as that of bands formed by UpC and DR4(II) probes (data not shown), to which one molecule of VDR/RXRα binds. This indicates that the lower band is the complex formed by the probe binding to one molecule of VDR/RXRα. As the amount of the protein was decreased, the intensity of the middle band (2× VDR/RXRα in Fig. 3B) decreased, while the intensity of the lower band remained constant. These results suggest that the middle band is the complex formed by the probe and two molecules of VDR/RXRα, and that three molecules of VDR/RXRα bind to this region with different affinities.

Furthermore, we performed EMSA in the presence of 1,25-$(OH)_2D_3$, which was required for the observation of three shifted bands (Fig. 3B), using longer probes containing at least one mutated half-site (Hs2, Hs6, and/or Hs8). These sites were shown to play an important role in DNA–VDR/RXRα complex formation in each segment, as shown in Fig. 2. The probes used for the EMSA are summarized in Fig. 3A. As shown in Fig. 3C, the upper bands in Fig. 3B disappeared when the M2, M4, and M12 probes were used; these probes each have one mutated half-site. In contrast, the M22, M23, and M30 probes, in which two of the three half-sites were mutated, caused the middle bands to disappear in addition to the upper bands.

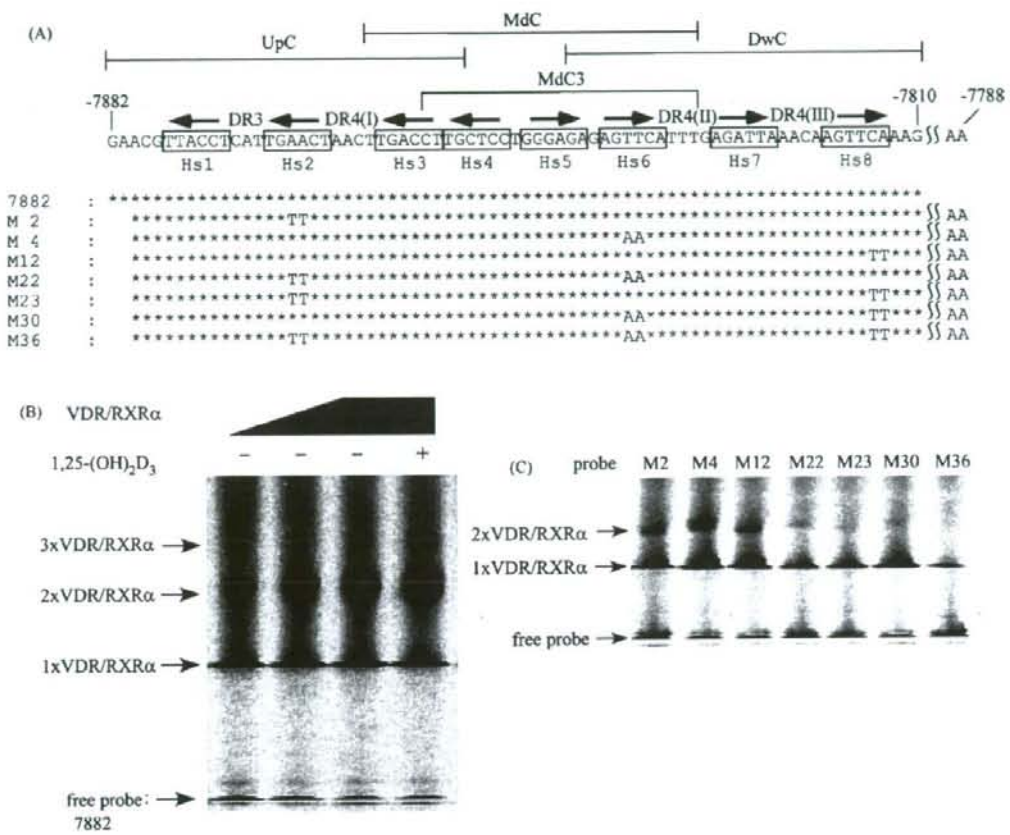

Fig. 3 – VDR/RXRα can bind to three VDR-binding sites at the same time. (A) The oligonucleotide sequences used for EMSA. Putative half-sites are boxed and arrows indicate the direction of the half-site. Numbers are in reference to the transcriptional start site at +1. Only nucleotides that differ from the wild-type are shown as letters; asterisks represent unchanged nucleotides. (B) EMSA was performed using a FITC-labeled 7882 probe. The probe was incubated with the increasing amount of in vitro translated VDR and RXRα as described in Section 2. The complexes were resolved by electrophoresis on a 2.8% Long Ranger gel. (C) EMSA was performed using several FITC-labeled probes, shown in (A). The probes were incubated with 1,25-$(OH)_2D_3$ and in vitro translated VDR and RXRα as described in Section 2. The complexes were resolved by electrophoresis on a 2.8% Long Ranger gel.

When all three half-sites were mutated (M36), the upper and middle bands disappeared and the lower band significantly decreased. These data indicate that one molecule of VDR/RXRα binds to each element including Hs2, Hs6, or Hs8. Consequently, three molecules of VDR/RXRα bind simultaneously to this region.

3.4. *VDR-binding sites located between −7880 and −7810 bp mediate the transactivation of MDR1 by 1,25-$(OH)_2D_3$*

In the experiments described above, we identified several VDR-binding sites. To test if these sites are functional, the same mutations introduced into the probes and competitors in the EMSA were introduced into the pMD*824Δ90L construct for use in the luciferase assay. The names of these mutants correspond to those used in the EMSA. The mutated regions of the constructs used for the luciferase assays are summarized in Fig. 4A. As shown in Fig. 4B, the mutation in Hs4 (M31) or Hs5 (M33), although slightly increased induction, had no apparent effect on inducibility, indicating that these half-sites play no significant role in induction by 1,25-$(OH)_2D_3$. The other mutations introduced into individual half-sites (M1, M2, M3, M4, M7, and M12) lead to decreased inducibility. The mutations introduced simultaneously into the two half-sites in two of the three segments resulted in a further decrease in induction by 1,25-$(OH)_2D_3$ (M28, M26, M29, M22, M27, M23, M30 in Fig. 4B). M22 and M29 (mutations in Hs2 and Hs6, and Hs3

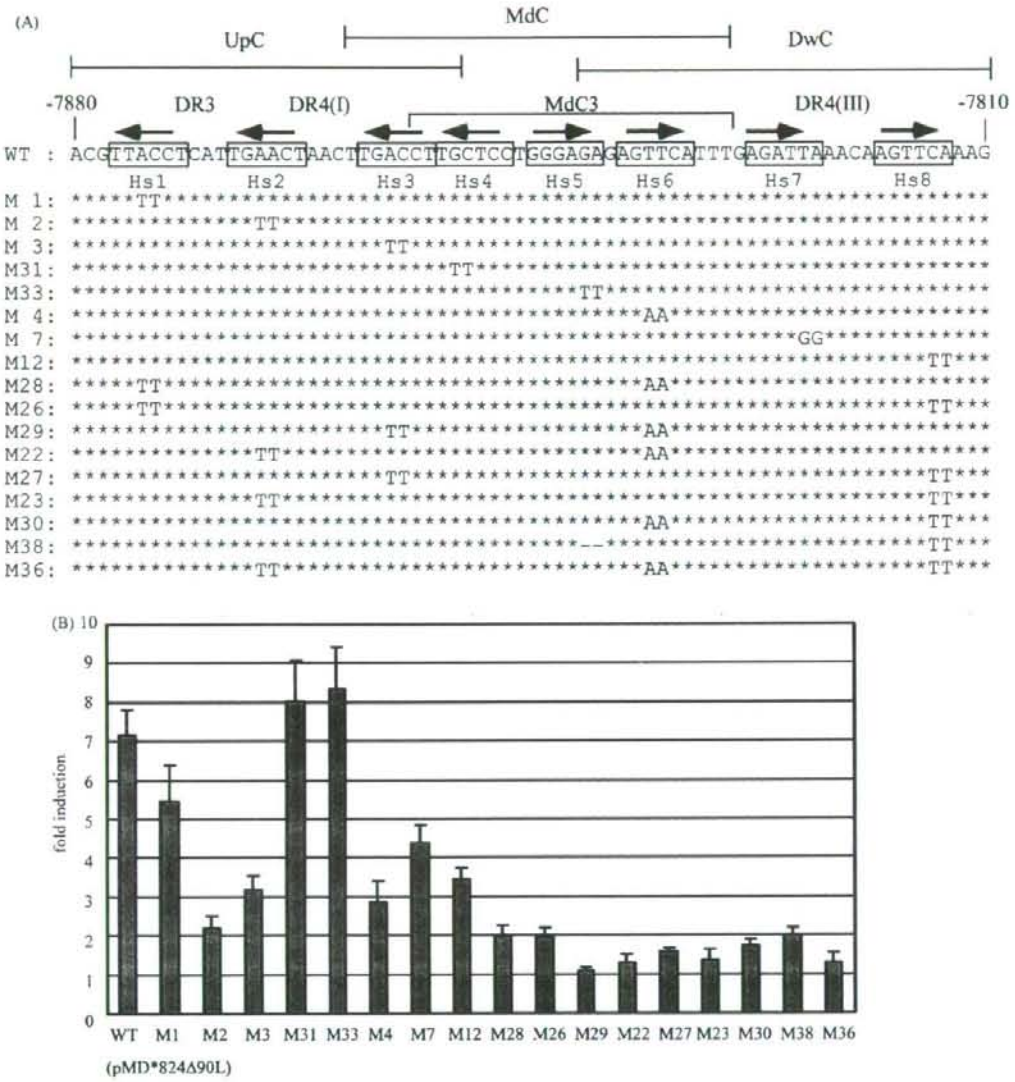

Fig. 4 – VDR-binding sites between −7880 and −7810 bp mediate the transcriptional activity of MDR1 by 1,25-$(OH)_2D_3$. (A) Several mutations were introduced into the pMD*824Δ90L plasmid (designated WT). Putative half-sites are boxed and arrows indicate the direction of the half-site. Asterisks denote bases identical to the wild-type sequence and letters indicate the bases altered in the mutated sequences. The underbar indicates deletion of a nucleotide. Numbers are in reference to the transcriptional start site at +1. (B) The luciferase activity was analyzed as described in Section 2. The fold induction was calculated as the radio of luciferase activity in 1,25-$(OH)_2D_3$-treated cells to that of DMSO-treated cells. Each value represents the mean ± S.D. of four independent experiments.

and Hs6, respectively) almost abolished inducibility. The inducibility of M38, which has the deletion of one of the three repeated AGs located between Hs5 and Hs6 in M12 (Fig. 4A), decreased more than that of M12 (Fig. 4B). The inducibility of M36, which has mutations in all three segments, was also almost abolished. These results indicate that every half-site in the VDR-binding sites, except Hs4 and 5, is a functional VDRE and makes its own contribution to induction by 1,25-$(OH)_2D_3$. Furthermore, each VDRE additively contributes to the 1,25-$(OH)_2D_3$ response.

4. Discussion

Several studies have shown that 1,25-$(OH)_2D_3$ induces the expression of MDR1 [7,22]. However, it remains unclear how 1,25-$(OH)_2D_3$ regulates MDR1 expression. In this study, we demonstrated that the induction of MDR1 by 1,25-$(OH)_2D_3$ is mediated by VDR/RXRα binding to the region located between −7.9 and −7.8 kbp upstream from the transcriptional start site of the human MDR1 gene (Fig. 5).

As shown in Fig. 1B, the region located between −7880 and −7817 bp is essential for VDR-mediated induction. This result is the same as that obtained for TR-mediated induction [19]. Furthermore, this region overlaps with the previously identified PXR-, CAR-responsive region [3,4]. The eight putative half-sites (Hs1–Hs8) of VDREs were found in the region located between −7880 and −7810 bp (Fig. 2A). DR3, DR4(I), DR4(II), and DR4(III), which were previously designated by Geick et al., are composed of Hs1 and Hs2, Hs2 and Hs3, Hs6 and Hs7, and Hs7 and Hs8, respectively. Geick et al. reported that PXR/RXRα bound to these three DR4, with the highest affinity to DR4(III), and DR4(I) is an important element for PXR-mediated induction [3]. Burk et al. reported that CAR bound to DR4(I) and DR4(III) as a heterodimer with RXRα, and to the 5′-half-site of DR4(II) (designated as Hs6 in this study) as a monomer [4]. As for transcriptional activity, DR4(I) and the 5′-half-site of DR4(II) were reported to be important elements for CAR-mediated induction. Recently, we reported that TR/RXRα bound to UpC [including DR3 and DR4(I)] and DwC [including DR4(II) and DR4(III)] segments [19], whereas TR/RXRα did not bind to MdC located between UpC and DwC (M. Saeki, K. Kurose, unpublished data). Furthermore, two molecules of TR/RXRα bind simultaneously to the region, and several DRs contribute to the binding affinity in the order: DR4(I) > DR4(II) > DR3 ≈ DR4(III). As for the transcriptional activity, every direct repeat contributes to TR-mediated induction [19]. In the present study, we showed that VDR/RXRα bound to UpC (including Hs1–3), MdC (including Hs3–6), and DwC (including Hs6–8) (Fig. 2B). To date, no nuclear receptors other than VDR has been reported to bind to MdC by forming heterodimers with RXRα. Although Hs6, which is located at the overlapping region between MdC and DwC, significantly contributes to induction by CAR [4], the binding of CAR/RXRα to MdC and contribution of MdC to induction by CAR remains to be elucidated. As shown in Fig. 2B, the relative binding affinity of the VDR-binding elements is DR4(I) > DR3 > MdC3 > DR4(III) > DR4(II). Consequently, the relative binding ability of VDR to these elements located in this region is clearly different from that of PXR, CAR, and TR, though the VDR-responsive region overlaps with the PXR-, CAR-, and TR-responsive regions [3,4,19]. The overlapping of nuclear receptor-responsive regions was also observed on the other genes such as CYP3A4 [23], in which PXR/RXRα and CAR/RXRα exhibited similar binding affinity toward proximal ER6 element [24]. On the nuclear receptor-responsive region of MDR1 gene, PXR/RXRα and CAR/RXRα bound to DR4(I) with similar affinity, although PXR/RXRα bound to DR4(III) with the higher affinity than CAR/RXRα [4]. Although, relative binding affinities among TR/RXRα, VDR/RXRα, PXR/RXRα, and CAR/RXRα to these binding elements have not been examined, it is conceivable that cooperative effects of the nuclear receptors with different binding affinities, tissue distributions and ligand concentrations affect the expression of MDR1.

Three shifted bands were observed when a longer probe including all the half-sites of the VDR-binding elements was used for EMSA (Fig. 3A). The upper band (3× VDR/RXRα) was found to be enhanced by 1,25-$(OH)_2D_3$. This has also been observed in VDREs located in several genes such as human CYP24 [25-27] and is due to the stabilization of DNA–VDR/RXRα formation by 1,25-$(OH)_2D_3$ [26,28,29]. The relative binding affinity of the VDR-binding elements estimated from Fig. 2B is DR4(I) > DR3 > MdC3 > DR4(III) > DR4(II). The affinity was examined further by using each discrete oligonucleotide as a competitor and a probe. Fig. 3 indicates that three molecules of VDR/RXRα bind simultaneously to the region, and one molecule of VDR/RXRα binds to each element including Hs2, Hs6, or Hs8. It is obvious that the element including Hs8 is DR4(III); consequently, the element including Hs6 is in MdC3, but it could not be specified further. Although both DR3 and

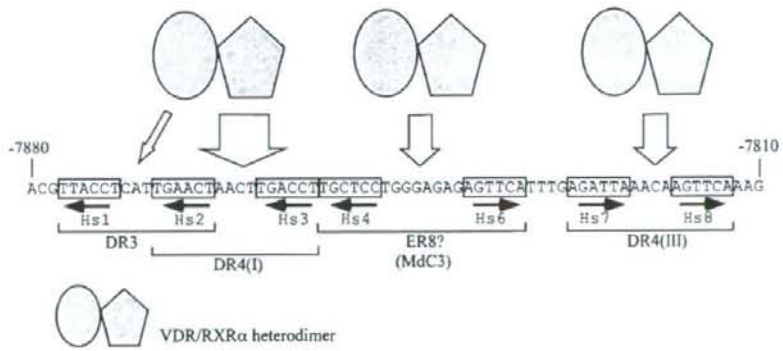

Fig. 5 – Three molecules of VDR/RXRα bind to VDREs located −7.9 to −7.8 kb upstream of the MDR1 gene with different affinities. The nucleotide positions are shown relative to the transcription start site of MDR1. The half-sites of the VDREs are boxed with arrows. VDR/RXRα binds to DR3 or DR4(I), ER8, and/or DR4(III) with different affinity, which is denoted by the thickness of the arrow.

DR4(I) include Hs2 and each alone shows high affinity to VDR/RXRα, two molecules of VDR/RXRα are not able to simultaneously bind to DR4(I) and DR3 because they overlap with Hs2 (Fig. 2A). Therefore, judging from the binding affinity and decreased inducibility from the reporter gene assay (Fig. 4B), three molecules of VDR/RXRα would mainly bind to DR4(I), MdC3, and DR4(III) simultaneously. The middle band intensity of the M4 probe (MdC3 mutation) was stronger than that of the M2 and M12 probes (DR4(I) and DR4(III) mutations, respectively) (Fig. 3C). The difference in the middle band intensity between the M4 and M12 probes in Fig. 3C suggests that the two molecules of VDR/RXRα simultaneously bind to DR4(I) and DR4(III) more strongly than to DR4(I) and MdC3, though the relative binding affinity of VDR/RXRα to MdC3 was higher than to DR4(III), as shown in Fig. 2B. The proximity of DR4(I) and MdC3 might slightly restrict the binding of the two molecules of VDR/RXRα to those sites simultaneously.

We confirmed whether the VDR-binding sites contribute to induction using constructs with mutations in several half-sites (Fig. 4). DR4(I) and DR4(III) contribute to induction by 1,25-$(OH)_2D_3$, and so are functional VDREs. MdC3 includes Hs4, Hs5, and Hs6. Although the mutation in Hs6 (M4) resulted in reduced inducibility, both the mutation in Hs4 (M31) and that in Hs5 (M33) had little effect on induction (Fig. 4B). Precisely which half-site is paired with Hs6 is unclear, but Hs6 contributes to induction by 1,25-$(OH)_2D_3$. However, when one AG deletion of the three repeated AGs, which are located just upstream of Hs6 (Fig. 4A), was introduced into M12, the inducibility of the resulting mutant construct M38 decreased more than that of M12 (Fig. 4B). This indicates that the deletion results in reduced inducibility, suggesting that the half-site paired with Hs6 is located upstream of Hs6, and that the change in the spacer length between Hs6 and its upstream partner leads to the reduced inducibility. Hs4 is located upstream of Hs6, and the mutation introduced in Hs4 reduced binding activity (Fig. 2C, Md3M31). Therefore, the partner of Hs6 might be Hs4, although the mutation of Hs4 alone did not reduced inducibility by 1,25-$(OH)_2D_3$ (Fig. 4B, M31). If Hs4 and Hs6 are partners, then they are an everted repeat by 8 nucleotides (ER8). The mutation in Hs1 (Fig. 4B, M1, M28, and M26), namely the mutation in DR3, caused somewhat decreased activity. Thus, DR3 can function as a VDRE, suggesting that DR3 serves as an auxiliary function of the neighboring DR4(I) element.

Double mutations in the different segments result in substantial reduction in induction by 1,25-$(OH)_2D_3$ (Fig. 4). Among them, the double mutations in DR4(I) and ER8 of MdC3 resulted in an almost complete loss of inducibility (M22 and M29 in Fig. 4B). In M22, only DR4(III) is a wild-type motif, and in M29, DR3 is a wild-type motif in addition to DR4(III). Therefore, DR4(III) alone or in combination with DR3 might be incapable of induction. However, DR4(III) works cooperatively in combination with DR4(I) and/or MdC3 (compare M2 with M23, M4 with M30, and WT with M12 in Fig. 4B). These results indicate that the additive binding of VDR/RXRα to several VDREs results in additional enhancement of MDR1 induction by 1,25-$(OH)_2D_3$.

Previous reports showed that Caco-2 cells are clearly less sensitive to the inductive effect of 1,25-$(OH)_2D_3$ compared with LS180 cells [7,30]. The VDR mRNA level in Caco-2 cells is lower than that in LS180 cells (twofold higher band intensity in LS180 cells) [9]. Additionally, the ligand-binding assay showed that LS180 and Caco-2 have VDR levels of 118 and 63 fmol/mg protein, respectively [31]. In our preliminary luciferase reporter experiment using LS180 cells transfected by pMD*824Δ90L, which contains VDREs, we observed transcriptional induction by 1,25-$(OH)_2D_3$ even in the absence of VDR expression plasmid (data not shown). Thus, the difference in response to 1,25-$(OH)_2D_3$ between these cells may reflect the amount of VDR/RXRα, which binds to the VDREs in the MDR1 gene. VDR is expressed abundantly in the human intestine (approximately 250 fmol/mg protein) [32,33]. Thus, it is possible that 1,25-$(OH)_2D_3$ is involved in intestinal MDR1 expression under normal physical conditions. Recent reports demonstrated that CYP27B1, which has an important role in the synthesis of 1,25-$(OH)_2D_3$, is expressed in human intestine [34–36]. In addition, extrarenally produced 1,25-$(OH)_2D_3$ primarily serves as an autocrine/paracrine factor with cell-specific functions [37,38]. Therefore, 1,25-$(OH)_2D_3$ levels in the intestine might be relatively high, whereas serum 1,25-$(OH)_2D_3$ levels are usually controlled at approximately 100 pmol/L. MDR1 expression levels are different between individuals [20], and these variations might affect the toxicity and efficacy of drugs. Intestinal vitamin D status, which might be affected by, for example, intestinal CYP27B1 and circulating 25-hydroxyvitamin D_3 levels, might partially contribute to differences between individuals in MDR1 expression.

Recently, it has been shown that 1,25-$(OH)_2D_3$ is involved in the formation of tight junctions, which seal the paracellular space between adjacent cells to create a primary barrier, in intestinal epithelial cells [39]. Kutuzova et al. reported that 1,25-$(OH)_2D_3$ causes increases in the expression of several phase I and phase II enzymes such as CYP3As in rat intestine after injection of 1,25-$(OH)_2D_3$ into vitamin D-deficient rats [40]. These data indicate that 1,25-$(OH)_2D_3$ would play an important role in the intestinal epithelial barrier function against xenobiotics by regulating tight junctions and inducing several drug-metabolizing enzymes and MDR1.

The induction of P-gp by 1,25-$(OH)_2D_3$ could lead to an increase in the systemic efflux of co-administrated drugs that serve as P-gp substrates. For instance, Olaizola et al. reported that the uptake of [^{99m}Tc]-sestamibi by the parathyroid glands of uremic patients was suppressed by pulse administration of 1,25-$(OH)_2D_3$ [13]. [^{99m}Tc]-Sestamibi is a substrate of P-gp and is excreted by P-gp [11,12], suggesting that P-gp induction by 1,25-$(OH)_2D_3$ leads to increased efflux of [^{99m}Tc]-sestamibi [13]. Vitamin D derivatives are widely prescribed, therefore, consideration for drug–drug interaction mediated by induction of P-gp by vitamin D derivatives should probably be paid.

In summary, we have demonstrated that the induction of MDR1 by 1,25-$(OH)_2D_3$ is mediated by VDR/RXRα binding to VDREs located between −7.9 and −7.8 kbp upstream of the human MDR1 gene, and that three molecules of VDR/RXRα are able to simultaneously bind with different affinities. DR3, DR4(I), MdC3 (ER8) and DR4(III) are functional VDREs, and the contribution of each VDRE toward inducibility is different (Fig. 5). Furthermore, each VDRE additively contributes to the 1,25-$(OH)_2D_3$ response.

Acknowledgements

We thank Dr. Shuichi Koizumi (Yamanashi University) for providing the human RXRα cDNA. This work was supported in part by grants from the Ministry of Health, Labor and Welfare of Japan and the Japan Health Sciences Foundation (Research on Publicly Essential Drugs and Medical Devices).

REFERENCES

[1] Marchetti S, Mazzanti R, Beijnen JH, Schellens JH. Concise review: clinical relevance of drug drug and herb drug interactions mediated by the ABC transporter ABCB1 (MDR1, P-glycoprotein). Oncologist 2007;12:927–41.
[2] Wacher VJ, Wu CY, Benet LZ. Overlapping substrate specificities and tissue distribution of cytochrome P450 3A and P-glycoprotein: implications for drug delivery and activity in cancer chemotherapy. Mol Carcinog 1995;13: 129–34.
[3] Geick A, Eichelbaum M, Burk O. Nuclear receptor response elements mediate induction of intestinal MDR1 by rifampin. J Biol Chem 2001;276:14581–7.
[4] Burk O, Arnold KA, Geick A, Tegude H, Eichelbaum M. A role for constitutive androstane receptor in the regulation of human intestinal MDR1 expression. Biol Chem 2005;386:503–13.
[5] Bertilsson G, Heidrich J, Svensson K, Asman M, Jendeberg L, Sydow-Backman M, et al. Identification of a human nuclear receptor defines a new signaling pathway for CYP3A induction. Proc Natl Acad Sci USA 1998;95:12208–13.
[6] Moore LB, Parks DJ, Jones SA, Bledsoe RK, Consler TG, Stimmel JB, et al. Orphan nuclear receptors constitutive androstane receptor and pregnane X receptor share xenobiotic and steroid ligands. J Biol Chem 2000;275:15122–7.
[7] Aiba T, Susa M, Fukumori S, Hashimoto Y. The effects of culture conditions on CYP3A4 and MDR1 mRNA induction by 1alpha,25-dihydroxyvitamin D(3) in human intestinal cell lines, Caco-2 and LS180. Drug Metab Pharmacokinet 2005;20:268–74.
[8] Pfrunder A, Gutmann H, Beglinger C, Drewe J. Gene expression of CYP3A4, ABC-transporters (MDR1 and MRP1–MRP5) and hPXR in three different human colon carcinoma cell lines. J Pharm Pharmacol 2003;55:59–66.
[9] Thummel KE, Brimer C, Yasuda K, Thottassery J, Senn T, Lin Y, et al. Transcriptional control of intestinal cytochrome P-4503A by 1alpha,25-dihydroxy vitamin D3. Mol Pharmacol 2001;60:1399–406.
[10] Patel J, Pal D, Vangal V, Gandhi M, Mitra AL. Transport of HIV-protease inhibitors across 1 alpha,25di-hydroxy vitamin D3-treated Calu-3 cell monolayers: modulation of P-glycoprotein activity. Pharm Res 2002;19:1696–703.
[11] Piwnica-Worms D, Chiu ML, Budding M, Kronauge JF, Kramer RA, Croop JM. Functional imaging of multidrug-resistant P-glycoprotein with an organotechnetium complex. Cancer Res 1993;53:977–84.
[12] Yamaguchi S, Yachiku S, Hashimoto H, Kaneko S, Nishihara M, Niibori D, et al. Relation between technetium 99m-methoxyisobutylisonitrile accumulation and multidrug resistance protein in the parathyroid glands. World J Surg 2002;26:29–34.
[13] Olaizola I, Zingraff J, Heuguerot C, Fajardo L, Leger A, Lopez J, et al. [(99m)Tc]-sestamibi parathyroid scintigraphy in chronic haemodialysis patients: static and dynamic explorations. Nephrol Dial Transplant 2000;15:1201–6.
[14] Drocourt L, Ourlin JC, Pascussi JM, Maurel P, Vilarem MJ. Expression of CYP3A4, CYP2B6, and CYP2C9 is regulated by the vitamin D receptor pathway in primary human hepatocytes. J Biol Chem 2002;277:25125–32.
[15] Schrader M, Nayeri S, Kahlen JP, Muller KM, Carlberg C. Natural vitamin D3 response elements formed by inverted palindromes: polarity-directed ligand sensitivity of vitamin D3 receptor-retinoid X receptor heterodimer-mediated transactivation. Mol Cell Biol 1995;15:1154–61.
[16] Tavera-Mendoza L, Wang TT, Lallemant B, Zhang R, Nagai Y, Bourdeau V, et al. Convergence of vitamin D and retinoic acid signalling at a common hormone response element. EMBO Rep 2006;7:180–5.
[17] Matilainen M, Malinen M, Saavalainen K, Carlberg C. Regulation of multiple insulin-like growth factor binding protein genes by 1alpha,25-dihydroxyvitamin D3. Nucleic Acids Res 2005;33:5521–32.
[18] Seoane S, Perez-Fernandez R. The vitamin D receptor represses transcription of the pituitary transcription factor Pit-1 gene without involvement of the retinoid X receptor. Mol Endocrinol 2006;20:735–48.
[19] Kurose K, Saeki M, Tohkin M, Hasegawa R. Thyroid hormone receptor mediates human MDR1 gene expression—identification of the response region essential for gene expression. Arch Biochem Biophys 2008;474: 82–90.
[20] Nakamura T, Sakaeda T, Ohmoto N, Tamura T, Aoyama N, Shirakawa T, et al. Real-time quantitative polymerase chain reaction for MDR1, MRP1, MRP2, and CYP3A-mRNA levels in Caco-2 cell lines, human duodenal enterocytes, normal colorectal tissues, and colorectal adenocarcinomas. Drug Metab Dispos 2002;30:4–6.
[21] Kurose K, Ikeda S, Koyano S, Tohkin M, Hasegawa R, Sawada J. Identification of regulatory sites in the human PXR (NR1I2) promoter region. Mol Cell Biochem 2006;281:35–43.
[22] Hochman JH, Chiba M, Nishime J, Yamazaki M, Lin JH. Influence of P-glycoprotein on the transport and metabolism of indinavir in Caco-2 cells expressing cytochrome P-450 3A4. J Pharmacol Exp Ther 2000;292: 310–8.
[23] Pascussi JM, Gerbal-Chaloin S, Drocourt L, Maurel P, Vilarem MJ. The expression of CYP2B6, CYP2C9 and CYP3A4 genes: a tangle of networks of nuclear and steroid receptors. Biochim Biophys Acta 2003;1619:243–53.
[24] Xie W, Barwick JL, Simon CM, Pierce AM, Safe S, Blumberg B, et al. Reciprocal activation of xenobiotic response genes by nuclear receptors SXR/PXR and CAR. Genes Dev 2000;14:3014–23.
[25] Lemplainen H, Molnar F, Macias Gonzalez M, Perakyla M, Carlberg C. Antagonist- and inverse agonist-driven interactions of the vitamin D receptor and the constitutive androstane receptor with corepressor protein. Mol Endocrinol 2005;19:2258–72.
[26] Toell A, Polly P, Carlberg C. All natural DR3-type vitamin D response elements show a similar functionality in vitro. Biochem J 2000;352(Pt 2):301–9.
[27] Kim S, Yamazaki M, Zella LA, Shevde NK, Pike JW. Activation of receptor activator of NF-kappaB ligand gene expression by 1,25-dihydroxyvitamin D3 is mediated through multiple long-range enhancers. Mol Cell Biol 2006;26:6469–86.
[28] Quack M, Carlberg C. Ligand-triggered stabilization of vitamin D receptor/retinoid X receptor heterodimer conformations on DR4-type response elements. J Mol Biol 2000;296:743–56.
[29] Kimmel-Jehan C, Jehan F, DeLuca HF. Salt concentration determines 1,25-dihydroxyvitamin D3 dependency of vitamin D receptor–retinoid X receptor–vitamin D-

responsive element complex formation. Arch Biochem Biophys 1997;341:75–80.
[30] Engman HA, Lennernas H, Taipalensuu J, Otter C, Leidvik B, Artursson P. CYP3A4, CYP3A5, and MDR1 in human small and large intestinal cell lines suitable for drug transport studies. J Pharm Sci 2001;90:1736–51.
[31] Shabahang M, Buras RR, Davoodi F, Schumaker LM, Nauta RJ, Evans SR. 1,25-Dihydroxyvitamin D3 receptor as a marker of human colon carcinoma cell line differentiation and growth inhibition. Cancer Res 1993;53:3712–8.
[32] Ebeling PR, Sandgren ME, DiMagno EP, Lane AW, DeLuca HF, Riggs BL. Evidence of an age-related decrease in intestinal responsiveness to vitamin D: relationship between serum 1,25-dihydroxyvitamin D3 and intestinal vitamin D receptor concentrations in normal women. J Clin Endocrinol Metab 1992;75:176–82.
[33] Kinyamu HK, Gallagher JC, Prahl JM, DeLuca HF, Petranick KM, Lanspa SJ. Association between intestinal vitamin D receptor, calcium absorption, and serum 1,25 dihydroxyvitamin D in normal young and elderly women. J Bone Miner Res 1997;12:922–8.
[34] Bises G, Kallay E, Weiland T, Wrba F, Wenzl E, Bonner E, et al. 25-Hydroxyvitamin D3-1alpha-hydroxylase expression in normal and malignant human colon. J Histochem Cytochem 2004;52:985–9.
[35] Tangpricha V, Flanagan JN, Whitlatch LW, Tseng CC, Chen TC, Holt PR, et al. 25-Hydroxyvitamin D-1alpha-hydroxylase in normal and malignant colon tissue. Lancet 2001;357:1673–4.
[36] Walters JR, Balesaria S, Khair U, Sangha S, Banks L, Berry JL. The effects of Vitamin D metabolites on expression of genes for calcium transporters in human duodenum. J Steroid Biochem Mol Biol 2007;103:509–12.
[37] Dusso AS, Brown AJ, Slatopolsky E. Vitamin D. Am J Physiol Renal Physiol 2005;289:F8–28.
[38] Hewison M, Burke F, Evans KN, Lammas DA, Sansom DM, Liu P, et al. Extra-renal 25-hydroxyvitamin D3-1alpha-hydroxylase in human health and disease. J Steroid Biochem Mol Biol 2007;103:316–21.
[39] Kong J, Zhang Z, Musch MW, Ning G, Sun J, Hart J, et al. Novel role of the vitamin D receptor in maintaining the integrity of the intestinal mucosal barrier. Am J Physiol Gastrointest Liver Physiol 2008;294:G208–16.
[40] Kutuzova GD, DeLuca HF. 1,25-Dihydroxyvitamin D3 regulates genes responsible for detoxification in intestine. Toxicol Appl Pharmacol 2007;218:37–44.

Archives of Biochemistry and Biophysics xxx (2008) xxx–xxx

Contents lists available at ScienceDirect

Archives of Biochemistry and Biophysics

journal homepage: www.elsevier.com/locate/yabbi

Thyroid hormone receptor mediates human *MDR1* gene expression—Identification of the response region essential for gene expression

Kouichi Kurose *, Mayumi Saeki, Masahiro Tohkin, Ryuichi Hasegawa

Division of Medicinal Safety Science, National Institute of Health Sciences, 1-18-1 Kamiyoga, Setagaya-ku, Tokyo 158-8501, Japan

ARTICLE INFO

Article history:
Received 30 December 2007
and in revised form 18 March 2008
Available online xxxx

Keywords:
P-glycoprotein (P-gp)
TR
Triiodothyronine (T3)
Thyroxine (T4)
Thyroid hormone response element (TRE)
ABCB1

ABSTRACT

P-glycoprotein, encoded by the *MDR1* gene, is a drug efflux transporter that is expressed in various tissues and plays an important role in the absorption and elimination of many drugs and xenobiotics. Induction of the *MDR1* gene affects drug disposition and the efficacy of drug treatment. In this study, we demonstrated that the thyroid hormone receptor (TR) induces *MDR1* gene expression in a thyroid hormone (TH)-dependent manner. The 5′-upstream region of the human *MDR1* gene was examined for the presence of TH-responsive elements. Luciferase-reporter gene assays revealed that the TH response region is located between −7.9 and −7.8 kb upstream from the transcription start site of *MDR1*. The region contains two TH response clusters, one of which includes a direct repeat with a three-nucleotide spacer (DR3) and a four-nucleotide spacer DR4(I), and the other of which includes two DR4s (II and III). Mutation analyses indicated that every direct repeat has a unique contribution to the TH response. In particular, DR4(I) was shown to be the most important element. Chromatin immunoprecipitation assays revealed that TR and retinoid X receptor (RXR) bind to the TH response region, and gel mobility shift assays confirmed that one molecule of TR/RXR heterodimer binds to each of the clusters in this region, with preferential binding to the upstream one. We furthermore demonstrated that two molecules of TR/RXR could bind simultaneously to the TH response region. The order of binding affinity to the direct repeats was DR4(I) > DR4(II) > DR4(III) ≈ DR3. Our results indicate that these two closely spaced TR/RXR-binding clusters are both required for the maximal induction of *MDR1* gene expression mediated by TR.

The *MDR1* (*ABCB1*) gene plays an important role in pharmacokinetics through the expression of efflux pump P-glycoprotein (P-gp)[1], which has a broad substrate specificity and tissue-specific distribution. P-gp is expressed at high levels on the apical/luminal surface of barrier (blood–brain barrier, intestine, placenta, blood–testis, and blood–ovarian barriers) and excretory (liver, kidney, adrenal gland) tissues, suggesting that P-gp can limit the cellular uptake of drugs into the brain, testis, fetus, and enterocytes and can eliminate drugs into the bile, urine, and intestinal lumen [1,2]. The expression of *MDR1* is induced by a variety of drugs, affecting pharmacokinetics and leading to a decrease in the systemic exposure of drugs that serve as P-gp substrates. The inducers, inhibitors, and tissue distribution patterns of P-gp and CYP3A4 overlap extensively, with the latter being the most abundantly expressed human cytochrome P450 that contributes to the metabolism of a wide spectrum of pharmaceutical drugs and xenobiotics [3,4]. Consequently, the expressions of *MDR1* and *CYP3A4* were expected to have similar induction mechanisms. In fact, the induction of both *MDR1* and *CYP3A4* was found to be mediated through transcriptional activation by the binding of nuclear receptors, such as pregnane X receptor (PXR) and constitutive androstane receptor (CAR), to distal enhancer elements located approximately 8 kb upstream from the transcription start sites of *MDR1* and *CYP3A4* [5–8].

In vivo drug transport can be radically changed by a variety of pathophysiological states, including thyroid dysfunction. For example, in patients with hyperthyroidism who are receiving digoxin—a well-known P-gp substrate—the renal clearance of digoxin is higher and the plasma concentration of digoxin is lower than after normalization of thyroid function [9]. P-gp expressed in the kidneys and intestine has a substantial effect on the urinary and plasma concentration of orally administered P-gp substrates. For example, the intestinal P-gp content is correlated with the AUC after the oral administration of digoxin [10]. Therefore, the alterations in the pharmacokinetics of digoxin in patients with hyperthyroidism can be explained by the induction of P-gp; in other words, the expression level of *MDR1* may increase in patients with hyperthyroidism which is characterized by higher levels of thyroid hormone. Siegmund et al. reported that the expression of intestinal

* Corresponding author. Fax: +81 3 3700 9788.
E-mail address: kurose@nihs.go.jp (K. Kurose).

[1] *Abbreviations used:* P-gp, P-glycoprotein; TH, thyroid hormone; TR, thyroid hormone receptor; DR, direct repeat; PXR, pregnane X receptor; CAR, constitutive androstane receptor; RXR, retinoid X receptor; TRE, thyroid hormone response element; UpC, upstream cluster; DwC, downstream cluster; CYP, cytochrome P450; MDR1, multidrug resistance 1; FITC, fluorescein isothiocyanate; ChIP, chromatin immunoprecipitation.

0003-9861/$ - see front matter © 2008 Elsevier Inc. All rights reserved.
doi:10.1016/j.abb.2008.03.020

P-gp increased after the oral administration of thyroxine (T4) in duodenal biopsy samples obtained from healthy human volunteers [11]. Mitin et al. demonstrated that T4 induced MDR1 mRNA and P-gp in human colon carcinoma cell lines [12]. Although these results indicate that thyroid hormone (TH) is involved in the induction of *MDR1* gene expression, there have been no direct evidence that the thyroid hormone receptor (TR) is involved in the induction.

THs, 3,5,3′-triiodothyronine (T3) and T4, modulate gene expression by interacting with thyroid hormone receptors (TRs), α and β, which are members of the nuclear receptor superfamily [13]. T3 is the principal active and main ligand of TR and is derived by the deiodination of T4. TRα and TRβ, encoded by two distinct genes—*THRA* (*NR1A1*) and *THRB* (*NR1A2*) [13,14], bind T3 and, with a lesser affinity, T4, and mediate TH-regulated gene expression. TR binds to TH-responsive element (TRE), typically as a heterodimer with retinoid X receptor (RXR). TREs consist of a direct repeat, an everted repeat, or an inverted repeat of the consensus hexamer (half-site) sequence of (G/A)GGT(C/G)A separated by a spacer that is several nucleotides long; in particular, DR4 (a direct repeat separated by four nucleotides) is a preferential site for TR binding [15].

Overt thyroid dysfunction is common in the general population [16]. Hypothyroidism is a common disorder affecting many people, especially those over the age of 60 years [17,18]. Patients with hypothyroidism are usually treated with TH replacement therapy. Since TH is widely prescribed and influences the induction of P-gp, which potentially affects pharmacokinetics, the role of TH in the mechanism of *MDR1* expression may be a worthwhile topic of study. In this study, we investigated the molecular mechanism of *MDR1* induction by TH using intestinal epithelial cell lines. We demonstrated that TR/RXR heterodimers bind to the TREs located −7.9 to −7.8 kb upstream from the transcription start site of *MDR1*, which is essential for the induction of *MDR1* by TH.

Materials and methods

Cell cultures and hormone treatment

Human intestinal epithelial cell lines LS180 and Caco-2 were obtained from American Type Culture Collection (Manassas, VA) and were routinely cultured in DME low-glucose medium D6046 (Sigma) containing 10% heat-inactivated fetal bovine serum (FBS), 1× nonessential amino acids (Life Technology), and penicillin (100 IU/ml)/streptomycin (100 μg/ml) (Life Technology) at 37 °C in a humidified atmosphere of 5% CO_2. To study the thyroid hormone actions, the medium was substituted with phenol red-free DME medium (Gibco, Invitrogen) supplemented with 10% dextran-coated charcoal-treated fetal bovine serum (Hyclone Inc.) for 24 h prior to treatment with vehicle (2 mM NaOH), L-thyroxine (T4, Sigma), 3,3′,5,-triiodo-L-thyronine (T3, Sigma), or 3,3′,5′,-triiodo-L-thyronine (rT3, Sigma). T4, T3, and rT3 stock solutions were prepared in 0.2 M NaOH and were added to the medium at a final concentration of 2 mM NaOH. For the time course experiments, LS180 cells were treated with T4 (5 μM) for 4–24 h followed by RNA preparation. For the concentration–response studies, LS180 cells were exposed to 0–1 μM T4, 0–25 nM T3, or 0–25 nM rT3 for 15 h followed by RNA preparation.

Quantitative reverse transcription-polymerase chain reaction (qRT-PCR)

At the end of the TH treatments, RNA and cDNA were prepared from cells using the Fastlane Cell cDNA Kit (Qiagen), following the manufacturer's instructions. The relative expression levels of MDR1, CYP3A4, and UGT1A1 mRNAs were measured using quantitative real-time PCR and the comparative C_t method, described by Applied Biosystems. The relative level of β-actin was also measured as an endogenous reference. The primers and probes for the MDR1, CYP3A4, and UGT1A1 cDNAs were all TaqMan Gene Expression Assays or Assays-on-Demand products from Applied Biosystems. For the normalization of the expression data, the Pre-Developed TaqMan Assay Reagents Endogenous Control human β-actin Kit (VIC-labeled probe; Applied Biosystems) was used. Real-time PCR was performed in 25-μl reactions using the Prism 7000 Sequence Detection System (Applied Biosystems), and the data were analyzed according to the manufacturer's guidelines. Each value represents the mean ± SD of four independent experiments. The fold induction was calculated relative to the untreated cells for each gene.

Plasmids

The *MDR1* 5′-flanking region (−10082/+117) was amplified using the TaKaLa LA PCR Kit (Takara) and genomic DNA prepared from LS180 cells as a template and the primer pairs 5′-CTGGTACCTTGTCATTGTTGAGAAGACGCTG-3′ and 5′-ACGCGTCGACG AACGGCCACCAAGACGTGAA-3′, which include the Kpn I and Sal I sites for cloning. The amplified fragment was digested by Kpn I and Sal I enzymes and ligated to the Kpn I/Xho I site of firefly luciferase rapid response reporter vector pGL4.12 (Promega), resulting in pMD10082L. The plasmids pMD7970L, pMD7145L, and pMD457L were constructed by deleting the Nhe I, Nhe I/Xcm I, and Sph I fragments from pMD10082L, respectively. pMD*824L was constructed by deleting the Xcm I/Sph I fragment from pMD7970L. pMD*824Δ90L, pMD*824Δ153L, and pMD*824Δ214L were constructed using pMD*824L as a template and the In-Fusion Dry-Down PCR Cloning Kit (Clontech) with a reverse common primer 5′-TCTG CAGTGGTCTTTCTTCAG-3′ and forward individual primers 5′-AAAAGGGGATGCTAG ACGTTACCTCATTGAACTAACTTGA-3′, 5′-AAAAGGGGATGCTAGGTTCAAAGTCTATGA ATCATAAAACGATAA-3′, and 5′-AAAAGGGGATGCTAGAGCTCTGCAATTCAAAAGCCA-3′, respectively.

Mutations at the half-sites of the direct repeats were introduced into the pMD*824Δ90L reporter plasmid using the Quick-Change Multi Site-Directed Mutagenesis Kit (Stratagene), according to the manufacture's instructions, with the following oligonucleotides used alone or in combination:

M1, 5′-AAGGGGATGCTAGACGTTTTCTCATTGAACTAACTTGAC-3′;
M2, 5′-GCTAGACGTTACCTCATTGTTCTAACTTGACCTTGCTCCTG-3′;
M3, 5′-GAACTAACTTGTTCTTGCTCCTGGG-3′;
M4, 5′-GACCTTGCTCCTGGGAGAGAGAACATTTGAGATTAAACAAG-3′;
M7, 5′-CCTGGGAGAGAGTTCATTTGAGATGGAACAAGTTCAAAGTCTATG-3′; and
M12, 5′-GAGAGAGTTCATTTGAGATTAAACAAGTTTTAAGTCTATGAATC-3′.

All the mutations were verified using DNA sequencing on an Applied Biosystems 3730 sequencer (Applied Biosystems). Human TRβ (TRβ1) cDNA in a pME18SFL3 vector was purchased from Toyobo Co., Ltd. EcoR I and Not I fragments, including the full-length TRβ cDNA, was subcloned into pcDNA3.1 (Invitrogen), resulting in the TRβ expression plasmid pcTRβ. The expression plasmid encoding human RXRα cDNA (pcDNA3.1-hRXRα) was a generous gift from Dr. Shuichi Koizumi (Yamanashi University, Japan).

Transient transfection and luciferase-reporter gene assays

Cells were seeded into 96-well plates and grown until 70–80% confluence, then transiently transfected using HilyMax transcription regent (Dojindo Laboratories, Japan) at a reagent:DNA ratio of 5:1, according to the manufacturer's instructions. One hundred nanograms/well of the luciferase-reporter plasmid to be examined was transfected with 10 ng/well of pcTRβ or pcDNA3.1 and 10 ng/well of pGL4.74 (Promega), a plasmid encoding the *Renilla reniformis* luciferase and used to normalize the transfection efficiency, in 100 μl/well of medium. Twenty-four hours after transfection, the cells were treated with 50 nM of T3. Firefly and *Renilla* luciferase activities were measured 3.5 h after treatment using the Dual-Glo Luciferase kit (Promega) in a Wallac 1420 ARVOsx Multilabel counter (PerkinElmer Life Science). The transfection efficiency of the firefly luciferase activity was normalized against the activity of the internal *Renilla* luciferase activity. The fold induction was calculated as a ratio of (the activity from T3-treated cells)/(the activity from untreated cells). Each value represents the mean ± SD of four independent experiments, in each of which the fold induction value was the ratio of the mean activity from four wells of T3-treated cells divided by the mean activity from four wells of untreated cells.

Chromatin immunoprecipitation (ChIP) assays

Caco-2 cells were transiently transfected with 6 μg/dish (100-mm) of pcTRβ and pcDNA3.1-hRXRα. After incubation for 40 h, the culture medium was changed to phenol red-free DME medium supplemented with 10% dextran-coated charcoal-treated fetal bovine serum. After incubation for 4 h, the cells were used for ChIP assays by using ChIP-IT Express Enzymatic Kit (Active Motif, Inc.) according to the manufacturer's instructions. Immunoprecipitation of the chromatin complexes were performed with an anti-human TRβ1 mouse monoclonal antibody (sc-738; Santa Cruz Biotechnology, Inc.) and anti-human RXRα mouse monoclonal antibody (PP-K8508-00; Perseus Proteomics, Inc.). As a negative control, anti-human PXR mouse monoclonal antibody (PP-H4417-00; Perseus Proteomics, Inc.) was used because PXR is not expressed in the Caco-2 cells. PCR was performed with 5 μl (from a total of 100 μl) of eluted immunoprecipitate or of 1.0% input (chromatin taken before immunoprecipitation) in a total volume of 25 μl for 30 cycles. The set of primers used for the amplification of −7886 to −7730 bp (TR-binding region) were: forward 5′-GAGTGAACGTTACCTCATTGAAC-3′ and reverse 5′-CCGAAATGGCTTTTG AATTG-3′. The set of primers used for the amplification of −9889 to −9762 bp (negative control region) were: forward 5′-AAATATGAGATGCATAGAGCC-3′ and reverse 5′-AACCTTCTTACTCTACTATAGTC-3′. Cycling conditions were 94 °C for 5 min, followed by 30 cycles at 94 °C for 15 s, 55 °C for 30 s, and 72 °C for 15 s. PCR products were resolved on 2.2% FlashGel DNA Cassettes (Lonza Rockland, Inc.).

Gel mobility shift assays

The upper strand sequences of the probes and competitors used in the gel mobility shift assays are shown in Figs. 4 and 5. The double-stranded oligonucleotide corresponding to the −218 to −117 region of the human *PXR* promoter [19] was used as the nonspecific competitor NS. The oligonucleotides that were used as probes and competitors were purchased from Sigma Genosys. Four longer probes of WT, M3, M7, and M21, containing the −7880 to −7788 region of the human *MDR1* gene (Fig. 5), were prepared by PCR amplification using the wild-type (pMD*824Δ90L) and its mutant plasmids (M3, M7, and M21) as templates, respectively, with 5′-fluorescein isothiocyanate (FITC)-labeled primers 5′-AGGGGATGCTAGACGT-3′ and 5′-TTATCGTTTTATGATTCATAGACTT-3′. The DNA fragments were purified using the GFX PCR DNA and Gel Band Purification Kit (GE Healthcare). The TNT T7 Quick Coupled Transcription/Translation System (Promega) was used for *in vitro* synthesis of human TRβ and RXRα proteins from the pcDNA3.1-based full-length cDNA expression plasmids, as recommended by the supplier. DNA–protein complexes were allowed to form by incubating 2.5-μl aliquots of the programmed lysates of TRβ or RXRα alone or mixed at a ratio of 1:1 or unprogrammed reticulocyte lysate with 0.5 μl of 0.33-μM 5′ FITC-labeled double-stranded oligonucleotide probe, 1 μl of 5× binding buffer (87.5 mM KCl, 20 mM $MgCl_2$, 0.5 mM EDTA, 2.5 mM DTT, 2.5 mM PMSF, 50% glycerol and 50 mM HEPES, pH 7.4), and 0.5 μl of 1 mg/ml poly(dI–dC) for 20 min at room temperature (Fig. 4). For the competition assays, the indicated amounts of unlabeled double-stranded competitor oligonucleotides were added simultaneously with the labeled probe. In the assays using the PCR-based probe (Fig. 5), 8 μl of the programmed reticulocyte lysates (TRβ and RXRα at a ratio of 1:2) were incubated with 0.5 μl of FITC-labeled probe, 1 μl of 10× binding buffer (30 mM $MgCl_2$, 1 mM EDTA, 5 mM DTT, 50% glycerol and 200 mM HEPES, pH 7.75), and 0.5 μl of 1 mg/ml poly(dI–dC) for 30 min at room temperature. An aliquot of the reaction mixture was electrophoresed on 4–7% Long Ranger gels (Cambrex) in 0.5× TBE (44.5 mM Tris, 44.5 mM boric acid, and 1.25 mM EDTA) at 500 V at room temperature on a slab gel DNA sequencer DSQ-2000 (Shimadzu).

Results

Thyroid hormone-mediated induction of MDR1

To investigate the induction of *MDR1* by thyroid hormone, an intestinal epithelial cell line, LS180, was used as a model cell line. Although MDR1 mRNA was reported to be induced by T4 (100 nM and 100 μM) after 72 h of exposure in LS180 V and Caco-2 cells [12], we were interested in examining the inducibility of MDR1 mRNA by T3 and T4 more minutely. When LS180 cells were treated with T4, the MDR1 mRNA was induced in a time- and dose-dependent manner (Fig. 1A and B). The relatively rapid induction implies that *MDR1* expression is regulated at the transcriptional level. The induction of *MDR1* was also observed in a T3 dose-dependent manner, but rT3, an inactive metabolite of T3, had no effect on the induction of the MDR1 mRNA (Fig. 1C). These results indicate that the expression of the *MDR1* gene is induced by thyroid hormones (THs) that are known to act through the thyroid hormone receptor (TR).

PXR and CAR, which are members of the nuclear receptor superfamily as well as TR, mediate the gene expression of some drug-metabolizing enzymes and transporters like *CYP3A4*, *UGT1A1*, and also *MDR1*. TR recognizes DNA motifs similar to PXR- or CAR-binding elements. Therefore, it is likely that *CYP3A4* and *UGT1A1* might be induced by TH. Unexpectedly, previous work demonstrated that the expression of *CYP3A4* was not induced by TH [12]. Thus, we examined the inducibility of *UGT1A1* expression by TH in addition to that of *CYP3A4*. As shown in Fig. 1B and C, both T4 and T3 failed to induce the gene expression of *UGT1A1* similar to *CYP3A4*.

Identification of thyroid hormone response region

To investigate the mechanism of *MDR1* gene expression induced by TH, we performed a luciferase-reporter gene assays, using the Caco-2 cell line to exclude the influence of PXR, because Caco-2 is an intestinal epithelial cell line as well as LS180 and expresses TR but not PXR, on the other hand, LS180 expresses both TR and PXR [12,20]. A genomic DNA fragment from −10 kb to +117 bp of the *MDR1* (the major transcription initiation site is designated as

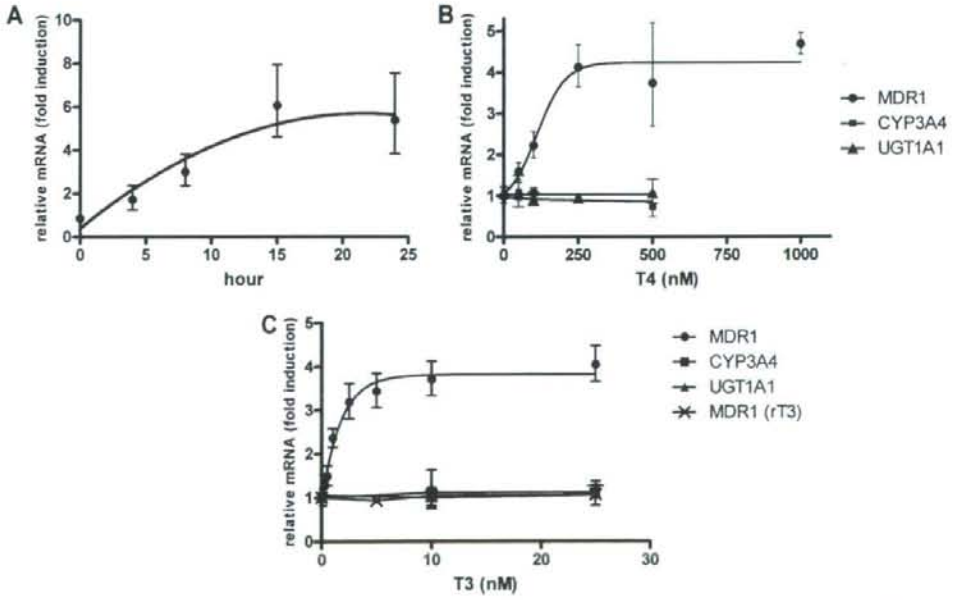

Fig. 1. Thyroid hormone-mediated induction of *MDR1* gene expression in LS180 cells. LS180 cells were treated with thyroid hormones followed by RNA preparation. The mRNA levels were analyzed by qRT-PCR as described in the Materials and methods section. The fold induction was calculated relative to the untreated cells for each gene. Each value represents the mean ± SD of four independent experiments. (A) Time course of T4-mediated induction of *MDR1* gene expression in LS180 cells. LS180 cells were treated with 5 μM T4 for 4, 8, 15, or 24 h followed by RNA preparation. (B) Effect of increasing the dose of T4 on the gene expressions of *MDR1*, *CYP3A4*, and *UGT1A1* in LS180 cells. LS180 cells were treated with 0–1000 nM T4 for 15 h followed by RNA preparation. (C) Effect of increasing the dose of T3 or rT3 on the gene expressions of *MDR1*, *CYP3A4*, and *UGT1A1* in LS180 cells. LS180 cells were treated with 0–25 nM of T3 or rT3 for 15 h followed by RNA preparation.

+1) was subcloned into a luciferase-reporter vector pGL4.12. In the absence of TR expression plasmid pcTRβ, the −10-kb-long construct showed just over a 2-fold induction by T3, as shown in Fig. 2A. By contrast, in the presence of pcTRβ, more than a 10-fold induction was induced by T3. These results indicate that TR mediates the TH response and that the TH response region is located within −10 kb to +117 bp of the *MDR1* gene. Similar results were obtained using LS180 cells (data not shown). To determine the TH response region, we constructed a variety of deletion mutants of *MDR1*-luciferase constructs and carried out a luciferase assay. As shown in Fig. 2A, a 5′-deletion from −7970 to −7145 led to a dramatic loss of inducibility by T3. The lost inducibility was recovered by the deleted region of 824 bp (Fig. 2A, bottom line). To specify the TH response region more precisely, a further 5′-deletion analysis of this 824 bp region was performed. As shown in Fig. 2B, more than a 90-bp deletion (to 153 and 214 bp) from the 5′-end of the 824 bp region caused the almost complete loss of T3 inducibility. Therefore, we concluded that the region between −7880 and −7817 is critical for the T3 response. As shown in Fig. 3A, this critical region includes AGGTCA-like repeats of one DR3 and three DR4(I, II, and III) motifs that are possible nuclear receptor binding sites. To investigate which motifs are responsible for the T3 response, mutant reporter plasmids in which 2-bp mutations were introduced in the half-sites of the direct repeats were constructed and assayed. As shown in Fig. 3A, the possible nuclear receptor response elements are composed of two clusters: the upstream one (UpC) contains DR3 and DR4(I), while the downstream one (DwC) contains DR4(II) and DR4(III). Each cluster also contains three half-sites in which the central half-site is shared by two direct repeats (DRs). Every mutation introduced in each half-site caused the loss of T3 induction to a varying degree (Fig. 3B, M1–M12). Especially, the M3 mutation that is located in the downstream half-site of DR4(I) caused a substantial decrease in inducibility. The double mutation introduced in each cluster (upstream and downstream) led to a much greater reduction than the single mutation (Fig. 3, M19–M23), indicating that every direct repeat makes its own contribution to the T3 response. In particular, DR4(I) seems to be a much more important element.

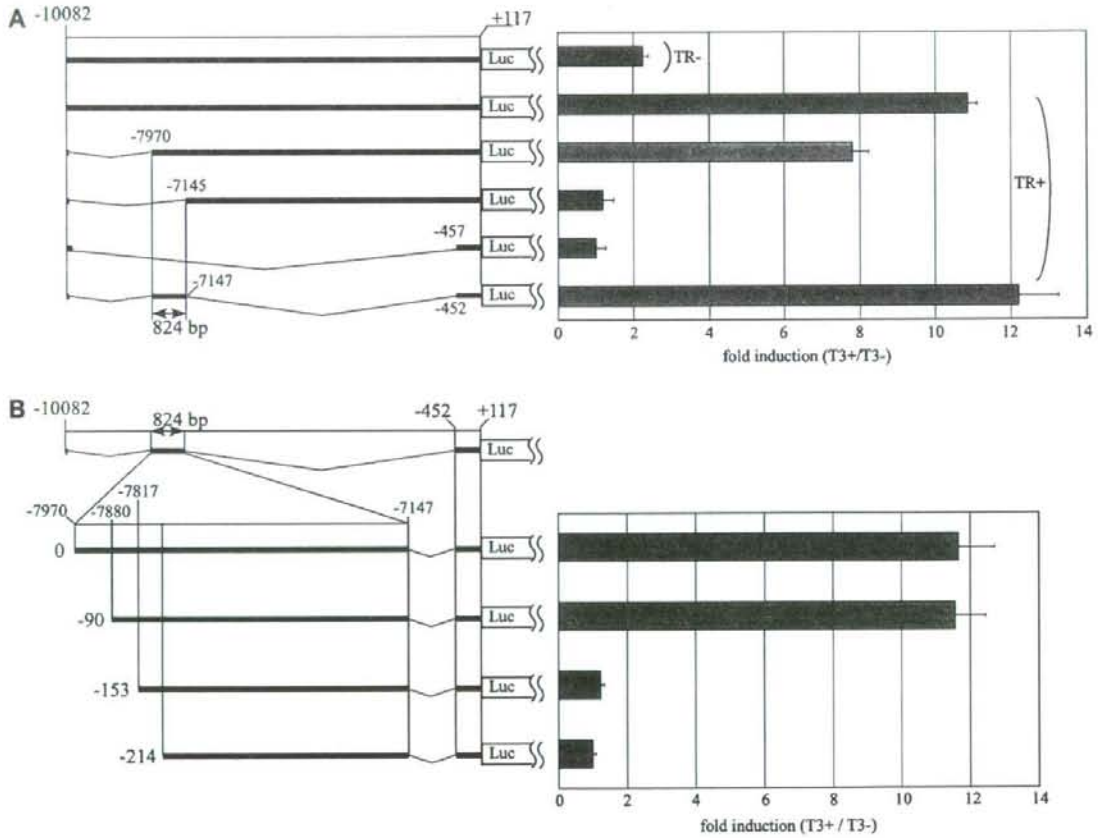

Fig. 2. Transcriptional activity of various *MDR1* 5′-deletion-luciferase-reporter constructs induced by T3 in transiently transfected Caco-2 cells. The luciferase activity was analyzed as described in the Materials and methods section. The fold induction was calculated as a ratio of (the activity from T3-treated cells)/(the activity from untreated cells) and is presented on the right side of each panel. Each value represents the mean ± SD of four independent experiments. The nucleotide positions in relation to the transcription start site are indicated. (A) Schematic presentations of the pMD10082L, pMD7970L, pMD7145L, pMD457L and pMD*824L are shown from the top of the left side. pMD10082L was introduced into the cells with pcDNA3.1 (TR-) or pcTRβ (TR+). The other constructs were introduced into the cells with pcTRβ (TR+). (B) Schematic presentations of pMD*824L, pMD*824Δ90L, pMD*824Δ153L, and pMD*824Δ214L are shown from the top of the left side.

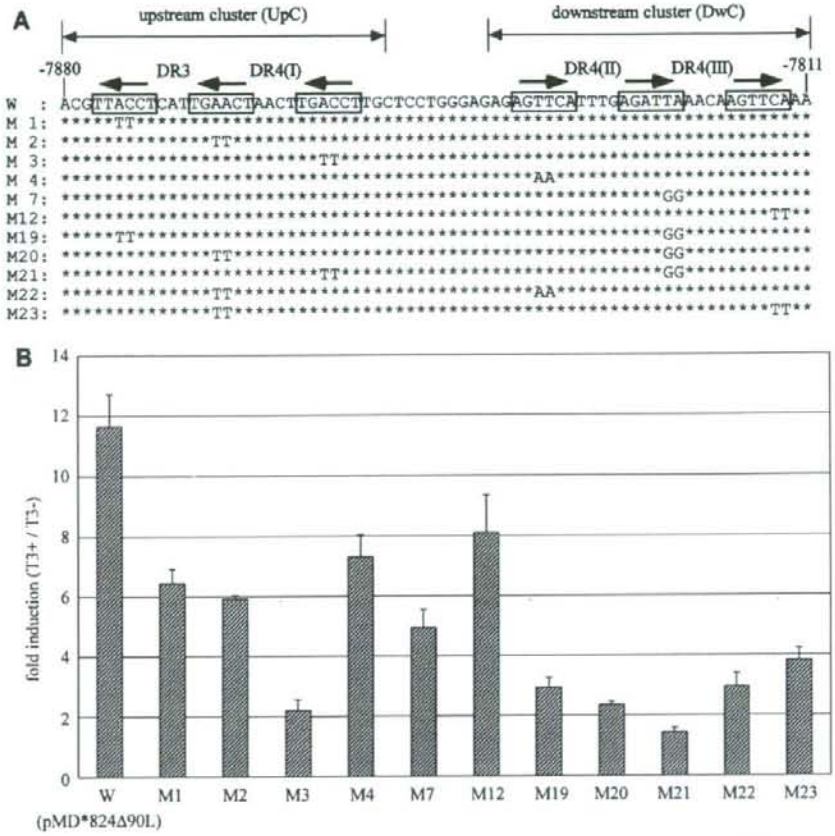

Fig. 3. Influence of different mutations in the thyroid hormone response region located between −7.9 and −7.8 kb upstream of the *MDR1* gene. (A) Based on the reporter plasmid pMD*824Δ90L (designated as W), various mutations were introduced in the half-sites of the direct repeats. The sequences from −7880 to −7811 (relative to the transcription start site of *MDR1*) of the reporter plasmid pMD*824Δ90L and the corresponding mutant plasmids (M1–M23) are indicated. The half-sites of the direct repeats are boxed with arrows that indicate the direction of the direct repeats. Nucleotides identical to the wild-type are shown as asterisks, and mutated nucleotides are shown as letters in the corresponding positions. (B) pMD*824Δ90L and corresponding mutant plasmids were introduced in Caco-2 cells with pcTRβ. The luciferase activity was analyzed as described in the Materials and methods section. The fold induction was calculated as a ratio of (the activity from T3-treated cells)/(the activity from untreated cells). Each value represents the mean ± SD of four independent experiments.

Binding of TR/RXR heterodimer to the thyroid hormone response region

We performed ChIP assays to examine whether TR and RXR are binding to the TH response region using Caco-2 cells transiently transfected with TR and RXR expression plasmids. Immunoprecipitations were performed using antibodies against TR, RXR, or control IgG. As shown in Fig. 4A, antibodies against TR and RXR, but not control IgG, immunoprecipitated the DNA fragments including TH response region. The negative control primers located 2 kb upstream of the TH response region, in which no possible TREs were found, produced no detectable PCR products except from input. These results indicate that TR and RXR are indeed binding to the TH response region in living cells and the TH response region is also TR binding region. We, therefore, hypothesized that the different levels of reduced inducibility in each mutation, as shown in Fig. 3, could be explained by differences in TR binding to the motifs in the thyroid hormone response region. To examine this possibility, we performed gel mobility shift assays using *in vitro* translated TRβ and RXRα to compare the binding affinities of TR/RXR heterodimer with DR3, DR4(I), DR4(II), and DR4(III) in the thyroid hormone response region. The probes and competitors used for the gel-shift assays are summarized in Fig. 4B. As shown in Fig. 4C and D, no protein–DNA complex was observed on any of the DNA motifs when unprogrammed reticulocyte lysates, TR only, or RXR only was used. As shown in Fig. 4C, TR/RXR formed a complex with the UpC probe including DR3 and DR4(I). The complex was eliminated by self-competition but not by nonspecific competition, indicating the sequence-specific binding of TR/RXR to the UpC. Using the DwC, including DR4(II) and DR4(III), as a competitor, the complex was also eliminated (but to a slightly lesser degree). Competitors of M1, M2, and M3 mutant oligonucleotides, including the same mutations as M1, M2, and M3 constructs used in the reporter gene assays in Fig. 3, respectively, inhibited complex formation in the following order: M1 > M2 > M3. In other words, the M3 mutation reduced the ability to form the TR/RXR–DNA complex most strongly. These results agree well with those obtained in the reporter gene assays, in which the M3 mutation strongly reduced transcriptional activation (Fig. 3). Each competitor of the four direct repeats in the thyroid hormone response region

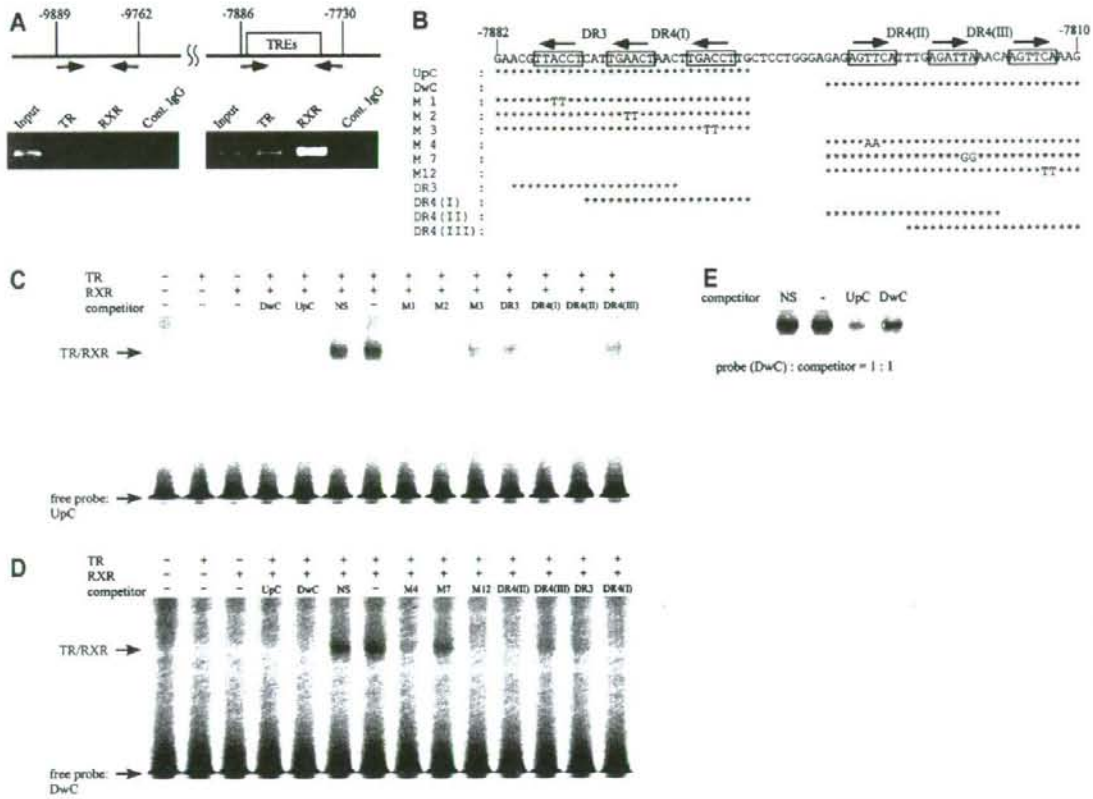

Fig. 4. TR/RXR heterodimer binds to direct repeats in the thyroid hormone response region. (A) TR and RXR binding to the TH response region detected by ChIP assays. The locations of the TH response region (TREs) and primer sets are shown at the top of the figure. Caco-2 cells transiently transfected with TRβ and RXRα expression plasmids were used for ChIP assays. As described in the Materials and methods section, ChIP assays were performed with antibodies against TRβ1, RXR, and control IgG. Input lanes indicate PCR products used soluble chromatin before immunoprecipitation as a template. (B) Oligonucleotide sequences used in the gel mobility shift assays. The nucleotide positions are shown relative to the transcription start site of *MDR1*. The half-sites of the direct repeats are boxed with arrows. Asterisks indicate nucleotides that are the same as the wild-type. (C) Gel mobility shift assay using *in vitro* translated proteins and an FITC-labeled oligonucleotide probe UpC. The labeled UpC probe was incubated with *in vitro* translated TRβ and/or RXRα or with unprogrammed reticulocyte lysate as a control in the presence or absence of a 20-fold molar excess of unlabeled oligonucleotides competitors. The complexes were resolved on a 7% Long Ranger gel. (D) Gel mobility shift assay using *in vitro* translated proteins and an FITC-labeled oligonucleotide probe DwC. The labeled DwC probe was incubated with *in vitro* translated TRβ and/or RXRα, or with unprogrammed reticulocyte lysate as a control in the presence or absence of a 15-fold molar excess of unlabeled oligonucleotides competitors. The complexes were resolved on a 7% Long Ranger gel. (E) Gel mobility shift assay using *in vitro* translated proteins and an FITC-labeled oligonucleotide probe DwC. The labeled DwC was incubated with *in vitro* translated TRβ and RXRα in the presence or absence of equimolar unlabeled oligonucleotide competitors. Complexes were resolved on a 6.5% Long Ranger gel. NS denotes nonspecific competitors, as described in the Materials and methods section.

inhibited the TR/RXR–UpC complex formation in the following order: DR4(I) > DR4(II) > DR3 ≈ DR4(III), as judged by the intensity of the gel-shift bands.

As in the case with the UpC probe, we carried out gel-shift assays with DwC, including DR4(II) and DR4(III), as a probe (Fig. 4D). The sequence-specific binding of TR/RXR to the DwC was confirmed using self- and nonspecific competitors. Mutations introduced into the M4, M7, and M12 competitors, which include the same mutations as the M4, M7, and M12 constructs used in the reporter gene assays, respectively, reduced the binding of TR/RXR, especially M7. These results also agree well with the results obtained in the reporter gene assays shown in Fig. 3. Every direct repeat competitor also competed with the DwC probe in forming a complex with a different affinity. Fig. 4E shows the competitive gel-shift assay with the DwC probe in which equimolar competitors of UpC or DwC were used. The binding affinity of TR/RXR to UpC was confirmed to be larger than that of DwC.

In summary, the TR/RXR heterodimer binds, with different affinity, to two clusters (UpC > DwC) and the DR motifs (DR4(I) > DR4(II) > DR4(III) ≈ DR3).

How many TR/RXR heterodimer molecules bind to the thyroid hormone response region?

We demonstrated that each cluster bound the TR/RXR heterodimer and demonstrated, using competitive gel-shift assays, that each direct repeat alone bound TR/RXR (Fig. 4C and D). Each cluster contains three half-sites in which the central half-site is shared by two direct repeats (Fig. 4B). Therefore, the question that arises is how many molecules of TR/RXR bind to each cluster including the two direct repeats. To examine this, we performed the gel mobility shift assay using the probe of DR4(II) as a representative of a direct repeat that binds one molecule of TR/RXR, in addition to the probes of UpC and DwC

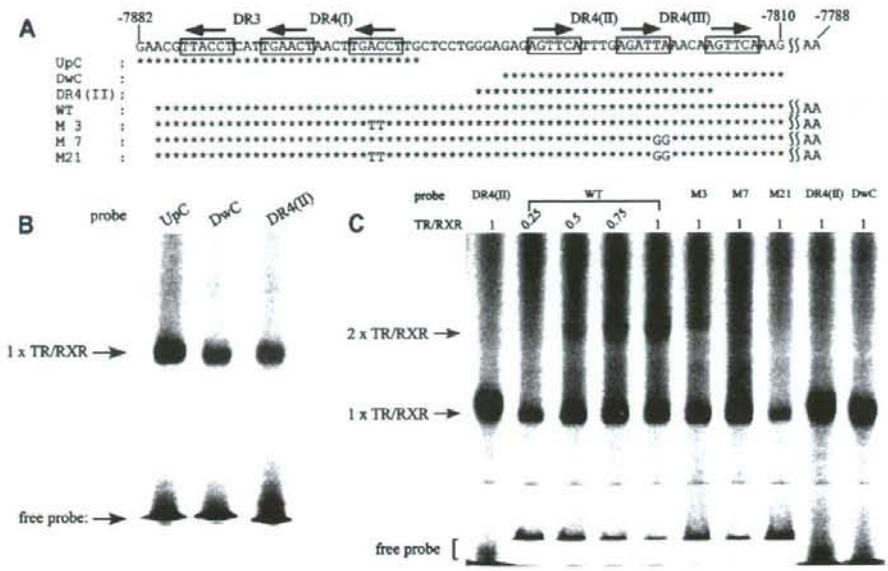

Fig. 5. Two molecules of TR/RXR heterodimer bind to the thyroid hormone response region. (A) Probes used in the gel mobility shift assays. The nucleotide positions are shown relative to the transcription start site of *MDR1*. The half-sites of direct repeats are boxed with arrows. Asterisks indicate nucleotides that are the same as the wild-type. (B) Gel mobility shift assay was performed using *in vitro* translated proteins and FITC-labeled oligonucleotide probes, as indicated. The labeled probes were incubated with *in vitro* translated TRβ and RXRα. The complexes were resolved on a 5% Long Ranger gel. (C) Gel mobility shift assay using *in vitro* translated proteins and the indicated FITC-labeled oligonucleotide probes. The labeled probes were incubated with the indicated amounts of *in vitro* translated TRβ and RXRα. The complexes were resolved on a 4% Long Ranger gel.

(Fig. 5). As shown in Fig. 5B, both UpC- and DwC–TR/RXR complexes exhibited the same mobility as that of the DR4(II)–TR/RXR complex, indicating that one molecule of TR/RXR binds to each cluster. Another question is how many molecules of TR/RXR bind to this region including the two clusters. Each cluster can bind one molecule, suggesting that two molecules of TR/RXR bind to this region, though the two clusters are spaced relatively close. Therefore, longer probes including the two clusters were used as gel-shift probes (Fig. 5A). As shown in Fig. 5C, one shifted band (primary band) was observed when a lower amount of TR/RXR was used with a wild-type longer probe (WT). The mobility of the band was the same as that from the DR4(II) and DwC probes, to which one molecule of TR/RXR binds. Increasing the amount of TR/RXR produced an increasing amount of a slower migrating secondary band that was thought to be a complex containing two molecules of TR/RXR (Fig. 5C). Although the primary bands were generated using M3 and M7 probes, the secondary bands were greatly decreased. Because the M3 and M7 probes contain mutations that reduced the binding of TR/RXR to UpC and DwC, respectively (Fig. 4), a single molecule of TR/RXR should bind to the other non-mutated clusters in both of the probes. Not only the secondary band, but also the primary band nearly disappeared when the M21 probe, which contains both M3 and M7 mutations, was used. These data strongly suggest that two molecules of TR/RXR can bind to this thyroid hormone response region (UpC and DwC) at the same time; at lower concentrations of TR/RXR, however, only one molecule of TR/RXR binds to the region (preferentially to UpC). These results coincide with those in the reporter gene assays, in which each of the M3 and M7 mutations alone could not suppress the transcriptional activation completely, while the M21 mutation abolished the activity (Fig. 3).

Discussion

In previous *in vivo* and *in vitro* studies, the expression of P-gp was induced by T4 [11,12,21,22]. The duodenal expression of P-gp and MDR1 mRNA increased in 8 healthy human volunteers after the oral administration of T4 for 17 days, although the induced level of mRNA was not statistically significant [11]. In rats, the expression levels of P-gp and mdr1a/1b mRNAs increased in a tissue-selective manner after the oral administration of T4 for 3 weeks [21,22]. In intestinal cell lines exposed to T4 for 72 h, MDR1 mRNA expression increased in LS180V cells, while the mRNA and P-gp levels increased in Caco-2 cells [12]. These data were obtained using a relatively long period of T4 exposure. The mechanism responsible for this induction, including whether P-gp was induced by TH directly or indirectly, remained uncertain. In the present study, we demonstrated that the induction of *MDR1* by TH is mediated by TR at the transcriptional level. We showed first the time- and dose-dependent induction of MDR1 mRNA by TH in LS180 cells (Fig. 1). Induction was observed after as few as 4 h, and rT3 had no effect on the induction, implying that the expression of *MDR1* was directly induced by TH through TR. We then conducted luciferase-reporter gene assays (Figs. 2 and 3), ChIP assays (Fig. 4), and gel-shift assays (Figs. 4 and 5), in which we demonstrated that the induction of *MDR1* gene expression by TH is transcriptionally regulated by TR through a TH response region located between −7.9 and −7.8 kb upstream of *MDR1*, including one DR3 and three DR4 motifs (Fig. 6). Previous studies have shown that PXR and CAR, members of the nuclear receptor superfamily as well as TR, mediate the up-regulation of *MDR1* through the response region located −7.9 to −7.8 kb upstream of the *MDR1* using an epithelial cell line LS174T [5,6]. The region responsive for TR was eventually found to be the same as that of PXR and CAR, however, the regulation manners of TR is different

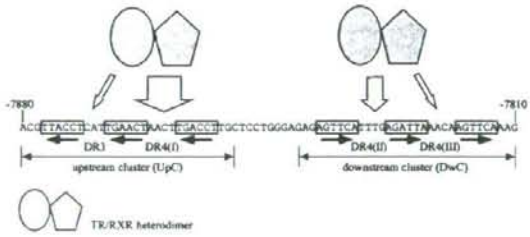

Fig. 6. Two molecules of TR/RXR bind to TH response region located −7.9 to −7.8 kb upstream of the *MDR1* gene with different affinities. The nucleotide positions are shown relative to the transcription start site of *MDR1*. The half-sites of the TREs are boxed. TR/RXR binds to DR3 or DR4(I), and/or DR4(II) or DR4(III) with different affinity, which is denoted by the thickness of the arrow.

from those of PXR and CAR. Geick et al. reported that PXR/RXR bound to three DR4 motifs with the strongest affinity to DR4(III) but did not bind to DR3 [6], whereas TR/RXR bound to all four TREs, including DR3, and bound to DR4(I) preferentially (Fig. 4). The binding affinity was in the following order: DR4(I) > DR4(II) > DR3 ≈ DR4(III) (Fig. 4). As for the transcriptional activity, DR4(I) was the most important element for PXR-mediated induction, similar to TR-mediated induction; however, DR4(III) mutation resulted in an increase in PXR induction [6], which differs from the case of TR. Burk et al. reported that CAR/RXR bound to DR4(I) and to a lesser degree to DR4(III) and that the CAR monomer, but not the CAR/RXR heterodimer, bound to DR4(II) [5]. The transcriptional activity at the region mediated by CAR is similar to that mediated by TR except that the DR4(III) mutation increased the induction by CAR as well as that by PXR. The transcriptional inducibility mediated by TR/RXR coincided with the TR/RXR-binding affinity to the DR motifs (Figs. 3–5). The DR motif with the largest contribution to the transactivation of *MDR1* by TR/RXR was DR4(I), and the other DR motifs likely serve as auxiliary engines for compensation. In recent years, regulatory proteins—including nuclear receptors—have been reported to cross-talk during the regulation of their target genes [23–27]. In this context, we examined the gene expressions of *CYP3A4* and *UGT1A1* by TH in LS180 cells (Fig. 1B and C). In addition to *MDR1* [5,6,28], the gene expressions of both *CYP3A4* and *UGT1A1* are induced by both nuclear receptors PXR and CAR [7,8,29–31], which recognize similar DNA motifs to those of TR. Unexpectedly, both T4 and T3 failed to induce the gene expressions of *CYP3A4* and *UGT1A1*, suggesting that TR is not involved in their gene regulation. Previously, Mitin et al. also reported that *CYP3A4* was not induced by TH. On the basis of the sequence comparison of a DR4 in the −8 kb region of *CYP3A4*, they speculated that the DR4 in *CYP3A4* might be nonfunctional for TR/RXR. Although each of TR, PXR, and CAR has its own manner of regulating *MDR1* expression, their mutual cross-talk may have enhancing or competitive effects on the *MDR1* transcription efficiency, which remains to be elucidated in the future.

Some drugs of P-gp substrates act as P-gp inhibitors that modulate P-gp function by competition for drug-binding sites or by blockading the ATP-hydrolysis process [1,2,32]. Amiodarone, an antiarrhythmic drug and a well-known competitive P-gp inhibitor, has been reported to decrease the activity of type I and type II 5′-deiodinases, which convert T4 to more potent T3 in peripheral tissues. This leads to a reduction in the production of T3, resulting in lower TH activity in the peripheral tissues [33,34]. In the present study, we demonstrated that TH induces *MDR1* mediated by TR. Therefore, this amiodarone-induced decrease in TH activity might also lead to reduced *MDR1* expression, which indirectly inhibits P-gp mediated by TR and might serve as another pathway for amiodarone-induced P-gp inhibition.

Verapamil, another antiarrhythmic drug and well-known P-gp inhibitor, was reported to inhibit TH efflux from several cell types, suggesting that P-gp is involved in TH efflux [35,36]. Mitchell et al. demonstrated that P-gp exports thyroid hormone from cells using specific inhibitors for P-gp (verapamil, nitrendipine, VX853, and VX710) and polarized MDCKII cells stably transfected with MDR1 cDNA [37]. Together with the presently reported results, these findings suggest that the induction of *MDR1* mediated by TR might serve as a feedback regulatory mechanism for TH homeostasis. This feedback loop is as follows: the expression of P-gp is induced by TH, causing the efflux of TH from cells through the induced P-gp, resulting in lower TH content in the cells, leading to reduction in P-gp expression by the reduced TH, resulting in the accumulation of TH in the cells by the reduced P-gp, inducing P-gp expression by the accumulated TH, causing the efflux of TH from the cells by the induced P-gp, and so on.

In summary, we demonstrated that the induction of *MDR1* gene expression by TH is mediated by TR through a TH response region located between −7.9 and −7.8 kb upstream from the transcription start site of *MDR1* (Fig. 6). This region contains two closely spaced TH response clusters, one of which is designated as UpC and includes a DR3 and a DR4(I), the other of which is designated as DwC and includes two DR4s(II and III). Every direct repeat makes its own contribution to the T3 response; in particular, DR4(I) was shown to be the most important element. TR formed a heterodimer with RXR at each of the UpC, DwC, and DR motifs, with preferential binding to DR4(I) in UpC. The binding affinity to the clusters was UpC > DwC, while that to the DR motifs was DR4(I) > DR4(II) > DR3 ≈ DR4(III). These results agreed well with the relative degree of contribution to the T3 response in transcriptional activity. Two molecules of the TR/RXR heterodimer could simultaneously bind to the TH response region including UpC and DwC, although one molecule of TR/RXR bound to the region (preferentially to DR4(I)) at lower concentrations of TR/RXR. Thus, the TH response region could be equipped with a booster system that is adapted to circumstances in which a higher concentration of ligand-bound TR/RXR exists.

Acknowledgments

We thank Dr. Shuichi Koizumi (Yamanashi University) for providing the human RXRα cDNA. This work was supported in part by grants from the Ministry of Health, Labor and Welfare of Japan and the Japan Health Sciences Foundation (Research on Publicly Essential Drugs and Medical Devices).

References

[1] J.H. Lin, Adv. Drug Deliv. Rev. 55 (2003) 53–81.
[2] S. Marchetti, R. Mazzanti, J.H. Beijnen, J.H. Schellens, Oncologist 12 (2007) 927–941.
[3] F.P. Guengerich, Annu. Rev. Pharmacol. Toxicol. 39 (1999) 1–17.
[4] F.P. Guengerich, Mol. Interv. 3 (2003) 194–204.
[5] O. Burk, K.A. Arnold, A. Geick, H. Tegude, M. Eichelbaum, Biol. Chem. 386 (2005) 503–513.
[6] A. Geick, M. Eichelbaum, O. Burk, J. Biol. Chem. 276 (2001) 14581–14587.
[7] B. Goodwin, E. Hodgson, D.J. D'Costa, G.R. Robertson, C. Liddle, Mol. Pharmacol. 62 (2002) 359–365.
[8] B. Goodwin, E. Hodgson, C. Liddle, Mol. Pharmacol. 56 (1999) 1329–1339.
[9] J. Bonelli, H. Haydl, K. Hruby, G. Kaik, Int. J. Clin. Pharmacol. Biopharm. 16 (1978) 302–306.
[10] B. Greiner, M. Eichelbaum, P. Fritz, H.P. Kreichgauer, O. von Richter, J. Zundler, H.K. Kroemer, J. Clin. Invest. 104 (1999) 147–153.
[11] W. Siegmund, S. Altmannsberger, A. Paneitz, U. Hecker, M. Zschiesche, G. Franke, W. Meng, R. Warzok, E. Schroeder, B. Sperker, B. Terhaag, I. Cascorbi, H.K. Kroemer, Clin. Pharmacol. Ther. 72 (2002) 256–264.
[12] T. Mitin, L.L. Von Moltke, M.H. Court, D.J. Greenblatt, Drug Metab. Dispos. 32 (2004) 779–782.
[13] F. Flamant, J.D. Baxter, D. Forrest, S. Refetoff, H. Samuels, T.S. Scanlan, B. Vennstrom, J. Samarut, Pharmacol. Rev. 58 (2006) 705–711.
[14] M.A. Lazar, Endocr. Rev. 14 (1993) 184–193.

[15] P.M. Yen, Physiol. Rev. 81 (2001) 1097–1142.
[16] K. Boelaert, J.A. Franklyn, J. Endocrinol. 187 (2005) 1–15.
[17] G.J. Canaris, N.R. Manowitz, G. Mayor, E.C. Ridgway, Arch. Intern. Med. 160 (2000) 526–534.
[18] M.P. Vanderpump, W.M. Tunbridge, J.M. French, D. Appleton, D. Bates, F. Clark, J. Grimley Evans, D.M. Hasan, H. Rodgers, F. Tunbridge, et al., Clin. Endocrinol. (Oxf) 43 (1995) 55–68.
[19] K. Kurose, S. Ikeda, S. Koyano, M. Tohkin, R. Hasegawa, J. Sawada, Mol. Cell. Biochem. 281 (2006) 35–43.
[20] K.E. Thummel, C. Brimer, K. Yasuda, J. Thottassery, T. Senn, Y. Lin, H. Ishizuka, E. Kharasch, J. Schuetz, E. Schuetz, Mol. Pharmacol. 60 (2001) 1399–1406.
[21] M. Jin, T. Shimada, M. Shintani, K. Yokogawa, M. Nomura, K. Miyamoto, Drug Metab. Pharmacokinet. 20 (2005) 324–330.
[22] N. Nishio, T. Katsura, K. Ashida, M. Okuda, K. Inui, Drug Metab. Dispos. 33 (2005) 1584–1587.
[23] J.M. Pascussi, S. Gerbal-Chaloin, L. Drocourt, P. Maurel, M.J. Vilarem, Biochim. Biophys. Acta 1619 (2003) 243–253.
[24] Y. Chen, G. Kissling, M. Negishi, J.A. Goldstein, J. Pharmacol. Exp. Ther. 314 (2005) 1125–1133.
[25] S. Kodama, C. Koike, M. Negishi, Y. Yamamoto, Mol. Cell. Biol. 24 (2004) 7931–7940.
[26] J. Sugatani, S. Nishitani, K. Yamakawa, K. Yoshinari, T. Sueyoshi, M. Negishi, M. Miwa, Mol. Pharmacol. 67 (2005) 845–855.
[27] E.S. Tien, M. Negishi, Xenobiotica 36 (2006) 1152–1163.
[28] T.W. Synold, I. Dussault, B.M. Forman, Nat. Med. 7 (2001) 584–590.
[29] J.M. Lehmann, D.D. McKee, M.A. Watson, T.M. Willson, J.T. Moore, S.A. Kliewer, J. Clin. Invest. 102 (1998) 1016–1023.
[30] W. Xie, M.F. Yeuh, A. Radominska-Pandya, S.P. Saini, Y. Negishi, B.S. Bottroff, G.Y. Cabrera, R.H. Tukey, R.M. Evans, Proc. Natl. Acad. Sci. USA 100 (2003) 4150–4155.
[31] J. Sugatani, H. Kojima, A. Ueda, S. Kakizaki, K. Yoshinari, Q.H. Gong, I.S. Owens, M. Negishi, T. Sueyoshi, Hepatology 33 (2001) 1232–1238.
[32] S.U. Sankatsing, J.H. Beijnen, A.H. Schinkel, J.M. Lange, J.M. Prins, Antimicrob. Agents Chemother. 48 (2004) 1073–1081.
[33] A.C. Bianco, D. Salvatore, B. Gereben, M.J. Berry, P.R. Larsen, Endocr. Rev. 23 (2002) 38–89.
[34] E. Martino, L. Bartalena, F. Bogazzi, L.E. Braverman, Endocr. Rev. 22 (2001) 240–254.
[35] F.A. Neves, R.R. Cavalieri, L.A. Simeoni, D.G. Gardner, J.D. Baxter, B.F. Scharschmidt, N. Lomri, R.C. Ribeiro, Endocrinology 143 (2002) 476–483.
[36] R.C. Ribeiro, R.R. Cavalieri, N. Lomri, C.M. Rahmaoui, J.D. Baxter, B.F. Scharschmidt, J. Biol. Chem. 271 (1996) 17147–17151.
[37] A.M. Mitchell, M. Tom, R.H. Mortimer, J. Endocrinol. 185 (2005) 93–98.